Phylogeny and revision of the '*Cubitermes* complex' termites (Termitidae: Cubitermitinae)

Working title: Phylogeny of *Cubitermes*

Simon Hellemans[1,2], Jean Deligne[3,4], Yves Roisin[2], Guy Josens[3]

[1]Okinawa Institute of Science & Technology Graduate University, 1919-1 Tancha, Onna-son, Okinawa 904-0495, Japan.

[2]Evolutionary Biology & Ecology, Université Libre de Bruxelles, Avenue F.D. Roosevelt 50, CP 160/12, B-1050 Brussels, Belgium.

[3]Laboratoire d'Écologie Végétale et Biogéochimie, Université Libre de Bruxelles, Avenue F.D. Roosevelt 50, CP 244, B-1050 Brussels, Belgium.

[4]Royal Museum for Central Africa, Entomology, Leuvensesteenweg 13, 3080 Tervuren, Belgium.

Correspondence: Hellemans Simon, Okinawa Institute of Science & Technology Graduate University, 1919-1 Tancha, Onna-son, Okinawa 904-0495, Japan; and Evolutionary Biology & Ecology, Université Libre de Bruxelles, Avenue F.D. Roosevelt 50, CP 160/12, B-1050 Brussels, Belgium. E-mail: simon.hellemans@gmail.com

ORCID references of authors

Simon Hellemans: 0000-0003-1266-9134

Jean Deligne: 0000-0002-4247-9270

Yves Roisin: 0000-0001-6635-3552

Guy Josens: 0000-0002-0887-4699

Abstract

The phylogeny of the genus *Cubitermes* Wasmann was reconstructed using two mitochondrial genes (*COI* and *COII*) and a fragment of the nuclear *28S rDNA*, including samples of *Apilitermes* Holmgren, *Crenetermes* Silvestri, *Megagnathotermes* Silvestri, and *Thoracotermes* Wasmann. Based on our analyses, we recovered these genera within a paraphyletic *Cubitermes* clade. *Cubitermes* species are distributed between five main clades, highly reflective of their enteric valve armatures (EVAs). Consequently, *Cubitermes* is here divided into five monophyletic genera based on phylogenetic analyses and EVAs: *Cubitermes* (*sensu stricto*), *Isognathotermes* Sjöstedt, *Nititidermes* Emerson, *Polyspathotermes* Josens & Deligne, **gen.n.**, and *Ternicubitermes* Josens & Deligne, **gen.n.** Moreover, the two species of *Megagnathotermes* included in this study, exhibiting different EVAs, are phylogenetically distant: *M. katangensis* Sjöstedt belongs in the genus *Polyspathotermes*, while *M. notandus* Silvestri remains as a monotypic genus. During the evolution of the *Cubitermes* complex, sclerotized EVA spatulae appeared twice independently: three or six spatulae in *Polyspathotermes* (*sulcifrons* and *oblectatus* patterns) and two jaw-like spatulae in *Nititidermes* (*sankurensis* pattern), which is absent in some species (*oculatus* pattern).

Zoobank registration: http://zoobank.org/urn:lsid:zoobank.org:pub:576AAFF8-63C6-4962-A8F5-75C9317AEA7B.

Key words: Blattodea; Dictyoptera; Ethiopian Region; Enteric valve; Mitochondrial DNA.

Introduction

Cubitermitinae is one of the eight subfamilies of the termite family Termitidae (Engel *et al.*, 2009) and contains 25 genera restricted to sub-Saharan Africa. Their gut anatomy is characterized by (*i*) a mixed segment separated from the ileum (P1) by a faint constriction; (*ii*) the enteric valve (P2) is funnel-shaped, not separated from P1, and bearing a characteristic armature; and (*iii*) a blind diverticulum, or caecum, occurring on the paunch (P3) (Noirot, 2001; Krishna *et al.*, 2013a). Within this subfamily, the soldiers of the genus *Cubitermes* Wasmann are characterized by sabre-like mandibles, a bifurcated labrum and presence of soil in the gut (Fig. 1 A). *Cubitermes* is one of the most diverse and abundant genera of African termites, and have successfully colonized various ecosystems from evergreen forests to rather dry savannahs (Williams, 1966). Some species build epigeal mushroom-shaped nests, which are typical of certain landscapes (Fig. 1 B-D). They play important ecological roles mainly through their action on the soil (Wood *et al.*, 1983; Okwakol, 1987; Donovan *et al.*, 2001b) and may be locally abundant (Wango & Josens, 2011). Krishna *et al.* (2013b) listed 67 valid species-group names, while Josens & Deligne (2019) proposed some new species and some invalid synonyms among the species that were synonymized by Ruelle (1975) and by Krishna *et al.* (2013b), bringing the number of species to 81. This figure might further increase if the genera *Megagnathotermes* Silvestri and *Nitiditermes* Emerson are found to be synonymous with *Cubitermes*, as suggested by Sands (1998).

As in the soldierless Apicotermitinae (Sands, 1972), the *Cubitermes* enteric valve armature (EVA), mainly of the worker caste, can be used for differentiating species groups (Josens & Deligne, 2019). In the subfamily Cubitermitinae, the basic enteric valve is a funnel bearing six elongated primary, prominent cushions of the valve (PC) alternating with non-prominent, secondary cushions of the valve (SCs) (Noirot, 2001). The cushions are armed with

cuticular outgrowths of different sizes and shapes: spines and bristles can be straight, bent, or even hooked.

Cubitermes workers feed on crude soil and display different types of fully developed enteric valves. Bouillon & Vincke (1971) mentioned the existence of at least three main kinds of EVA in the genus *Cubitermes*, with or without sclerotized spatulae. Josens & Deligne (2019) distinguished nine species groups on the basis of their EVA. Six of them are variations on the basic EVA, but three of them, namely the *sankurensis*, *oblectatus*, and *sulcifrons* groups are characterized by the presence of two, three, and six sclerotized spatulae on the PC, which project from the valve into the paunch (P3). Note that *Nititermes berghei* Emerson and *Megagnathotermes katangensis* Sjöstedt respectively possess two and three such spatulae as well (Sands, 1998; plate 10: fig. 6; plate 11: fig. 5). One of the main conclusions from Josens & Deligne (2019) is that several species may have soldiers with similar external morphologies, which used to make *Cubitermes* so difficult to identify, but may possess different types of EVA. A brief overview of EVA is given in Table 1 (modified from Josens & Deligne, 2019: table 4).

Bouillon & Vincke (1971) suggested that EVAs might reflect different diets, although all *Cubitermes* species are basically soil feeders and considered to belong to the feeding group IV of Donovan *et al.* (2001a). A link between diet differentiation and EVA is indeed supported by the fact that two or three species can occupy the same niche habitat at high densities (Williams, 1966; Wango & Josens, 2011), and when this happens, the coexisting species display different EVA. Moreover, two coexisting *Cubitermes* species with different EVA display different isotopic signatures, probably reflecting the consumption of soil at different levels (Josens & Wango, 2019).

Few species of *Cubitermes* have hitherto been sequenced for molecular phylogenetic studies. In a limited area around the Lopé reserve in Gabon, Roy *et al.* (2006) found that *Cubitermes* sp. aff. *subarquatus* Sjöstedt represented four cryptic species. Inward *et al.* (2007)

included two unidentified *Cubitermes* species in their phylogenetic study. They considered the *Cubitermes* group (= Cubitermitinae) to be monophyletic (based on 13 sampled genera). They also recovered *Cubitermes, Crenetermes* Silvestri, and *Thoracotermes* Wasmann in an unresolved clade with *Apilitermes* Holmgren as the sister group. Bourguignon *et al.* (2017) examined the historical biogeography of 11 Cubitermitinae genera, including seven *Cubitermes* species. They concluded that Cubitermitinae evolved around 30 Mya during the early Oligocene and are endemic to Africa, and that *Thoracotermes macrothorax* (Sjöstedt), *Apilitermes longiceps* (Sjöstedt) and *Crenetermes albotarsalis* (Sjöstedt) were included within the *Cubitermes* clade. Here, we consider that the *Cubitermes* complex comprises the genera *Cubitermes, Apilitermes, Crenetermes, Megagnathotermes, Nititditermes* and *Thoracotermes*.

The taxonomy of *Cubitermes* complex genera has been obscured by many inadequately detailed historical descriptions. A first step in modernising the taxonomic concepts of this genus was to split it into nine species groups according to their EVA (Josens & Deligne, 2019). Whether or not these groups should be raised to generic rank remains subjective although genetic data helps discriminate groups of related taxa. In the context of this limited morphological and genetic background, the objectives of this paper are to (*i*) establish a comprehensive phylogeny of the *Cubitermes* complex, (*ii*) investigate whether the nine species groups based on EVA (*sensu* Josens & Deligne, 2019) are consistent with their phylogeny and thus predicating any robust species level revision; (*iii*) organize the present genus *Cubitermes* accordingly into natural groups (e.g., genera); and (*iv*) assess the monophyly of *Megagnathotermes* and *Nititditermes* relative to *Cubitermes* as suggested by Sands (1998).

Materials and Methods

Biological samples

Termites were collected either into pure ethanol or RNA-later® from various localities across West and Central Africa, including Benin, Burkina Faso, Burundi, Cameroon, Central African Republic, Congo, Côte d'Ivoire, DRC (Haut-Katanga, Kinshasa and Tshopo provinces), Gabon and Senegal. Termites were identified to species using Sjöstedt (1926) and Williams (1966) and by comparison with type specimens. A total of 56 samples of the *Cubitermes* complex were selected for molecular analyses so as to maximize the number of species and their geographic distribution, including samples of *Apilitermes longiceps, Crenetermes albotarsalis, Megagnathotermes notandus* Silvestri*, M. katangensis*, and *Thoracotermes macrothorax*. Five species were added as outgroups for phylogenetic reconstructions: (*i*) Macrotermitinae: *Macrotermes amplus* (Sjöstedt) —replacement name for *M. muelleri* (Sjöstedt) (see Krishna *et al.*, 2013b: 1024), (*ii*) Cubitermitinae: *Furculitermes parviceps* Emerson and *Procubitermes aburiensis* Sjöstedt, as well as (*iii*) Neotropical Termitinae: *Cavitermes tuberosus* (Emerson) and *Palmitermes impostor* Hellemans & Roisin (Table S1).

Enteric valves (Fig. 2) were dissected and mounted on microscope slides. Images of slide preparations were obtained with a Zeiss Discovery V12 stereomicroscope equipped with an AxioCam ICc3 camera and controlled by AxioVision software. Images are each compilations of a series of successive stepwise-focussed photographs.

Phylogenetic reconstruction

We reconstructed the phylogeny of the termite genus *Cubitermes* using two mitochondrial genes, cytochrome oxidase I (*COI*) and II (*COII*), and a fragment of the nuclear ribosomal gene *28S rDNA*. Details of molecular procedures are provided in Supplementary Methods (Section SM-1), with cycling conditions in Table S2. From the initial 61 samples, all were successfully

amplified for *COII* and *28S rDNA*, and 54 for *COI*. All sequences have been deposited in GenBank under accessions MN646697 to MN646750 for *COI*, MN685897 to MN685956 for *COII*, and MN685957 to MN686017 for *28S rDNA* (see Supplementary Table S1 for details).

Bayesian Inferences (BI) were performed on the combined data in order to infer the species tree from two separate datasets: (*i*) 61 samples for which we obtained both *COII* and *28S rDNA*, and (*ii*) 54 samples for which all genes were obtained. For both analyses, each gene was aligned individually using the MUSCLE algorithm (Edgar, 2004) implemented in CodonCode Aligner. In the first analysis, alignments consisted in 61 sequences of 685 and 894 bp, with 278 and 160 polymorphic sites respectively for *COII* and *28S rDNA*. In the second analysis, alignments consisted in 54 sequences of 657, 685, and 894 bp, with 294, 277, and 154 polymorphic sites respectively for *COI*, *COII*, and *28S rDNA*. The best nucleotide-substitution models with the lowest Bayesian Information Criterion (BIC) were determined as TPM2uf+G for *COI*, TrN+I+G for *COII,* and TVM+I+G for *28S rDNA* for both analyses using jModelTest v2.1.10 (Darriba *et al.*, 2012). Phylogenetic analyses with BI were performed using the software BEAST v2.5.1 (Bouckaert *et al.*, 2014) with the method StarBEAST2 (Ogilvie *et al.*, 2017). Gene trees were modelled under strict molecular clocks with nucleotide-substitution models determined above. For the three-gene analysis, *COI* and *COII* trees were linked to account for the transmission of the mitochondrial sequences as one single locus. A Yule speciation process was modelled by setting the population mean to 1/X with a uniform speciation rate. Markov Chain Monte Carlo (MCMC) analyses were run for 30 million generations, sampling every 10,000 generations, and a burn-in of 10%, leaving a total of 5,400 trees. We followed traces with Tracer v1.7.1 (Rambaut *et al.*, 2014) to ensure that all effective sample sizes (ESS) of estimated parameters were above 200. Resulting ultrametric phylogenetic trees were reconstructed as maximum clade credibility trees with mean node heights using TreeAnnotator v2.5.1 (Bouckaert *et al.*, 2014) and visualized using FigTree v1.4.3 (Rambaut, 2017).

Mitochondrial and nuclear trees were mirrored using the 'cophyloplot' function from the ape package (Paradis *et al.*, 2004) in *R* v3.5.1 (*R* Development Core Team, 2018).

We also carried out BI on *COII* using the 61 sequences obtained in this study, as well as 13 previously published sequences retrieved from GenBank (see Table S3; Roy *et al.*, 2006; Bourguignon *et al.*, 2015; Bourguignon *et al.*, 2017). Taxonomic identity of *Cubitermes* samples, from which published sequences originated, was re-evaluated following Josens & Deligne (2019) (Table S3). The 75 sequences were aligned using the MUSCLE algorithm (Edgar, 2004) implemented in CodonCode Aligner, resulting in an alignment of 685 bp with 281 polymorphic sites. The best nucleotide-substitution model was HKY+I+G according to the BIC using jModelTest v2.1.10 (Darriba *et al.*, 2012). BI was undertaken with MrBayes v3.2.7 (Ronquist *et al.*, 2012), using two parallel runs, each consisting in four simultaneous MCMC of 10 million generations, sampling every 5,000 generations and discarding the first 20% samples from the cold chain as a burn-in. Convergence was ensured by checking that average standard deviation of split frequencies between the two runs was below 0.01, and all ESS were above 200. The resulting non-ultrametric consensus tree was visualized using FigTree v1.4.3 (Rambaut, 2017).

Phylogenetic analyses and reconstruction of trait states

The following analyses were conducted on the three-gene analysis, excluding distant outgroups (*i.e.*, *Macrotermes amplus*, *Cavitermes tuberosus*, and *Palmitermes impostor*). We performed a Mantel test (Mantel, 1967) between genetic and geographic distance to test for the presence of recent gene flow; a positive correlation would indicate the absence of gene flow, contrary to a near-zero correlation. Matrices of pairwise genetic distances of both mitochondrial (*COI* and *COII*) and nuclear (*28S rDNA*) DNA were obtained using the Kimura 2-parameter model (Kimura, 1980) implemented in MEGA X (Kumar *et al.*, 2018). Geographic distances were

computed as spherical (Vincenty, 1975) using the geosphere package in *R* (Hijmans, 2019). Mantel tests were performed using 9,999 permutations with the *ade4* package in *R* (Dray & Dufour, 2007).

Mesquite v3.6 (build 917) (Maddison & Maddison, 2019) was used in order to better understand the evolution of morphological traits, using the best resolved BI tree. Traits used for reconstruction were: (*i*) the nine worker EVA types (see Table 1 A) *sensu* Josens & Deligne (2019), and (*ii*) soldier labrum shape. Ancestral states were reconstructed under a parsimony model with unordered characters for each trait, minimizing the switches along the tree.

Results

Phylogenetic analyses

Overall, the topologies of phylogenetic trees were consistent among outgroups in both the two and three-gene StarBEAST2 analyses (61 and 54 sequences respectively). However, the topology was better resolved amongst internal nodes (*i.e.,* supported by higher Bayesian Posterior Probabilities (BPP) values) in the three-gene analysis. Therefore, only phylogenetic trees of the three-gene analyses are considered in the following sections (Figs 3, S1 A-C; see Fig. S2 A-D for trees from the two-gene analyses). Mantel tests on samples from the subfamily Cubitermitinae (three-gene dataset, *i.e.* 51 samples) revealed some structure of the genetic diversity for the mitochondrial loci ($r = 0.161$, $p < 0.01$) but none for the nuclear one ($r = 0.003$, $p = 0.47$).

Topologies of mitochondrial (1,342 bp; linked *COI* and *COII*; Fig. 3) and nuclear (894 bp; *28S rDNA*; Fig. S1 A) trees were not congruent (Fig. S1 B; see Fig. S2 C for the two-gene analysis) with the latter not recovering prior species-level concepts. This was notably the case for *C. proximatus* (Fig. S1 A) and *C. sankurensis* (Fig. S2 B) which were split into several clades. Furthermore, most internal nodes of the mitochondrial tree were highly resolved (BPP > 0.95), while those of the nuclear tree were characterized by lower BPP. The total evidence tree (Fig. S1 C) exhibited the same topology (although with lower BPP support values) as the mitochondrial one, except for the position of *Megagnathotermes notandus* and *Th. macrothorax*. Consequently, the results below are mainly described with respect to the highly resolved mitochondrial tree (Fig. 3).

Based on the results of the mitochondrial and nuclear trees, as well as the total evidence tree, *A. longiceps*, *Cr. albotarsalis*, *M. notandus*, and *Th. macrothorax* were included within the *Cubitermes* clade (Figs 3; S1A-C; S2A-D). Considering both the mitochondrial and the total evidence trees, *Cubitermes* species were distributed between five main clades, highly reflective

of EVA groups, described hereafter according to separation events. (*i*) The first clade was composed of two species with a *bilobatus* EVA (*C. exiguus* Mathot and *C. tenuiceps* (Sjöstedt)) with *Apilitermes* as sister group. (*ii*) The second consisted of seven species, six with a *sankurensis* EVA (*C. orthognathus* (Emerson), *C. proximatus* Silvestri, *C. sankurensis* Wasmann, *C. schereri* (Rosen), and two undescribed species), within which an undetermined species with an *oculatus* EVA was nested. (*iii*) The third combined species with either a *fungifaber* EVA (*C. fungifaber* (Sjöstedt), *C. severus* Silvestri, and *C. ugandensis* Fuller) or a *finitimus* EVA (*C. finitimus* Schmitz, *C. planifrons* Sjöstedt, and two undescribed species) into a sister group to *Crenetermes*. (*iv*) The fourth comprised five species with either a *sulcifrons* EVA (*C. bugeserae* Bouillon & Vincke, *C. inclitus* Silvestri, *C. sulcifrons* Wasmann, and an undescribed species) or an *oblectatus* EVA (*M. katangensis*). (*v*) The fifth was constituted of three species with a *bilobatodes* EVA (*C. bilobatodes* Silvestri, *C. weissi* Silvestri, and an undetermined species, see Fig. S2 A,D) within which two species with a *muneris* EVA (*C. muneris* (Sjöstedt) and *C. pallidiceps* (Sjöstedt)) were nested.

Finally, it is to be highlighted that the two species of *Megagnathotermes* included in this study, exhibiting different EVAs, were separated within the *Cubitermes* clade: *M. katangensis* was grouped with *sulcifrons* EVA species, while *M. notandus*, showing affinities with *Th. macrothorax* (BPP = 0.98; Fig. 3), was established as the sister group of clades III-IV-V detailed above (BPP = 0.97; Fig. 3).

Classification

After EVA and morphology examination, it appeared that the four cryptic species assigned to '*Cubitermes* sp. *aff. subarquatus*' in Roy *et al.* (2006) belonged to two groups. (*i*) '*Cubitermes* spA' and '*Cubitermes* spD' (GenBank accessions DQ127302 and DQ246541, respectively; Table S3) displayed the *fungifaber* EVA and matched the morphology of *C. fungifaber*. (*ii*)

'*Cubitermes* spB' and '*Cubitermes* spC' (DQ127312 and DQ127306, respectively) possessed a *finitimus* EVA; *C. subarquatus* is probably a junior synonym of *C. finitimus* (Emerson *in* Krishna *et al.*, 2013b: 1938). While 'spB' matched well the *C. planifrons* morphology, 'spC' was very close to the *C. finitimus* morphology but was definitely different on a genetic basis (this is truly a cryptic species). Phylogenetic reconstruction on the *COII* alignment with MrBayes confirmed the assignment of 'spA' and 'spD' to *C. fungifaber* and 'spB' to *C. planifrons*, while 'spC' was established as a sister group of *C. fungifaber* (Fig. 4; Table S3).

Additionally, seven *Cubitermes* samples for which entire mitogenomes were sequenced previously (Bourguignon *et al.*, 2015, 2017), were morphologically re-examined (for details, see Table S3). The taxonomic assignment of DJ 0091 (KY224661) and DJ 0676 (KY224606) to *C. ugandensis* and *C. sulcifrons,* respectively, was confirmed, as their *COII* sequences clustered with other conspecific samples (Fig. 4). DJ 0183 (KY224600), identified nominally as *C.* nr. *fulvus,* was confirmed as *C. fulvus* Williams and also grouped with the other species with a *sankurensis* EVA based on *COII* (Fig. 4). Contrary to Bourguignon *et al.* (2017) who identified DJ 0186 (KY224421) as *C. fulvus* Williams, we identified it here as *C. bugeserae* (Fig. 4). The sample CA1 with accession KP026265, assigned to *C. fungifaber* by Bourguignon *et al.* (2015), was re-identified as a species belonging to the *finitimus* EVA group based on photographs; based on its *COII* sequence it formed a clade with the sample 'spC' from Roy *et al.* (2006), as the sister group to *C. fungifaber* (Fig. 4). DJ 0620 (KY224569), labelled as '*Cubitermes* sp. A', was identified as *C. finitimus*; we similarly recovered it clustered with the other members of this species on the *COII* tree (Fig. 4). Finally, DJ 0093 (KY224475) was identified as *C. oblectatus* by Bourguignon *et al.* (2017) but was here re-assigned to *C.* sp. aff. *katangensis*.

*Taxonomic status of the '*Cubitermes *complex*'

Our results showed that enteric valve armature patterns (or EVAs), as defined in Josens & Deligne (2019), were supported as five major clades and that the genera *Apilitermes*, *Crenetermes*, *Megagnathotermes*, and *Thoracotermes* were nested within a paraphyletic *Cubitermes*. It follows that the genus *Cubitermes* is here split into five monophyletic genera, defined according to the major clades and EVAs. These five genera share these same morphological characters in soldiers: presence of a diverticulum on the paunch, presence of soil in their gut (dark abdomen), cubic to cuboid head capsule bearing a dense bunch of bristles around and above fontanelle, bifurcated labrum, reaping mandibles from almost straight to evenly curved or even more or less hooked, each one bearing a small marginal tooth near the molar tooth, and fore, mid and hind tibiae bearing 3, 2, 2 apical spurs and 0, 2, 0 subapical spurs respectively. Full descriptions of these genera will be provided in the ongoing revisions, together with identification keys to the species level. Here, we provide diagnostic characters at the genus level, *i.e.* the characteristics of the workers' EVAs (see Table 1 A). Species to be included in the various genera are designated according to combinations recently in use (as in Krishna *et al.*, 2013b). A list of described taxa considered as currently valid (following Josens & Deligne, 2019; this work) is given below for each genus as well as in Supplementary Table S4 with their authority.

Taxonomy

Genus *Cubitermes* Wasmann

Type species: *Termes bilobatus* Haviland, 1898: 411-412; by original designation.

Diagnosis. The workers within this genus have basic *bilobatus* EVAs, with nearly triangular primary cushions (see Table 1 and Fig. 2 A).

Species included (9). *C. bilobatus* (Haviland) (synonym: *C. bilobatus curtus* Sjöstedt), *C. conjenii* (Fuller), *C. exiguus* Mathot, *C. pretorianus* Silvestri, *C. pretorianus heidelbergi* Fuller,

C. sanctaeluciae (Fuller), *C. tenuiceps* (Sjöstedt), *C. transvaalensis* (Fuller), *C. zulucola* Sjöstedt (synonym: *C. pseudoduplex* (Fuller)).

Etymology. From Latin *cubus*, cube; and *termes*, termite. Refers to the cubic or cuboid shape of the soldiers' heads.

Comments. This genus corresponds to the clade I in this work and to the *bilobatus* pattern in Josens & Deligne (2019).

Genus *Isognathotermes* Sjöstedt

Type species: *Eutermes (Cubitermes) minitabundus* Sjöstedt, 1913: 368-369; by original designation.

Diagnosis. The odd-numbered PCs of worker's enteric valve bear either crests or bulges in their downstream part (see Table 1 and Fig. 2 D,E).

Species included (15). *I. bulbifrons* (Sjöstedt) (synonym: *I. heghi* (Sjöstedt)), *I. congoensis* (Emerson), *I. finitimus* (Schmitz) (synonyms: *I. loubetsiensis* (Sjöstedt), *I. subarquatus* (Sjöstedt)), *I. fungifaber* (Sjöstedt) (synonyms: *I. banksi* (Emerson), *I. comstocki* (Emerson), *I. schmidti* (Emerson)), *I. gaigei* (Emerson), *I. gibbifrons* (Sjöstedt), *I. kemneri* (Emerson), *I. minitabundus* (Sjöstedt), *I. modestior* (Silvestri), *I. planifrons* (Sjöstedt) (suspected synonym: *I. fungifaber elongatus* (Sjöstedt)), *I. severus* (Silvestri), *I. silvestrii* (Sjöstedt), *I. speciosus* (Sjöstedt), *I. ugandensis* (Fuller) (synonym: *I. antennalis* (Sjöstedt)), *I. zenkeri* (Desneux).

Etymology. From Greek *ισος*, *isos*, equal, even; *γναθος*, *gnatho*s, mandible; and Latin *termes*, termite. Probably refers either to the resemblance between both mandibles, or to the fact that their diameter varies little between both ends, as it is the case in the type species *I. minitabundus*.

Comments. This genus was considered a junior synonym of *Cubitermes* since Snyder's catalog (1949); here, we restore it as valid. It corresponds to the clade III in this work and to the *fungifaber* and *finitimus* patterns in Josens & Deligne (2019).

Genus *Nititidermes* Emerson

Type species: *Nititidermes berghei* Emerson, 1960: 10-12; by original designation.

Diagnosis. In most of the species (grouping the *sankurensis* EVA), the worker has an enteric valve with two PCs (PC3 and PC4) ending downstream in two yellow to brown sclerotized spatulae which look like two jaws ("*valvule à mâchoires*" in Bouillon & Vincke, 1971; see Table 1 and Fig. 2 G). However, in two species (of the *oculatus* pattern), the workers have basic enteric valves i.e. without any spatulae (see Table 1 and Fig. 2 F).

Species included (15). *N. aemulus* (Silvestri), *N. anatruncatus* (Fuller), *N. berghei* Emerson, *N. curtatus* (Silvestri), *N. fulvus* (Williams), *N. niokoloensis* (Roy-Noël), *N. oculatus* (Silvestri), *N. orthognathus* (Emerson), *N. proximatus* (Silvestri), *N. sankurensis* (Wasmann) (synonyms: *N. cubicephalus* (Sjöstedt), *N. sankurensis elongatus* (Sjöstedt), *N. sibitiensis* (Sjöstedt)), *N. schereri* (von Rosen), *N. sierraleonicus* (Sjöstedt), *N. testaceus* (Williams), *N. truncatoides* (Fuller) (synonym: *N. truncatoides sordwana* (Fuller)), *N. truncatus* (Holmgren) (synonym: *N. duplex nduma* (Fuller)).

Etymology. From Latin *nitidus*, shiny; and *termes*, termite. Clearly refers to the shiny appearance of the imago's tegument and soldier's mandibles pointed out by Emerson in the specific case of the type species *N. berghei*.

Comments. This genus corresponds to the clade II in this work and to the *oculatus* and *sankurensis* patterns in Josens & Deligne (2019).

Genus *Polyspathotermes* Josens & Deligne, gen.n.

http://zoobank.org/urn:lsid:zoobank.org:act:563784CA-7CA6-4923-BAE2-0634A186436F

Type species: *Cubitermes sulcifrons* Wasmann, 1911: 156-158.

Diagnosis. Two worker enteric valve patterns are found within this group: either with three PCs (PC3, PC4, and PC5) ending downstream in yellow to brown sclerotized spatulae or with all six PCs ending in sclerotized spatulae (see Table 1 and Fig. 2 H,I).

Species included (8). *P. bugeserae* (Bouillon & Vincke), *P. inclitus* (Silvestri) (synonym: *P. domifaber* (Sjöstedt)), *P. intercalatus* (Silvestri) (synonym: *P. hamatus* (Sjöstedt)), *P. katangensis* (Sjöstedt), *P. montanus* (Williams), *P. oblectatus* (Harris), *P. sulcifrons* (Wasmann), *P. umbratus* (Williams).

Etymology. From Greek *πολυς*, *polus*, many; and *σπαθος, spathos*, spatula. Refers to the morphology of EVAs, in which more than two cushions bear sclerotized spatulae. Gender: masculine.

Comments. This genus corresponds to the clade IV in this work and to the *oblectatus* and *sulcifrons* patterns in Josens & Deligne (2019); it includes *Megagnathotermes katangensis*.

Genus *Ternicubitermes* Josens & Deligne, gen.n.

http://zoobank.org/urn:lsid:zoobank.org:act:D3850221-F28D-4527-8345-D5E2477C41BF

Type species: *Cubitermes bilobatodes* Silvestri, 1912: 247-249.

Diagnosis. The workers within this genus have basic EVAs, with fusiform or roughly rectangular primary cushions (see Table 1 and Fig. 2 B,C).

Species included (13). *T. bilobatodes* (Silvestri), *T. breviceps* (Sjöstedt), *T. duplex* (Holmgren), *T. falcifer* (Williams), *T. glebae* (Sjöstedt), *T. latens* (Williams), *T. microduplex* (Fuller), *T. muneris* (Sjöstedt) (synonym: *T. bisulcatus* (Sjöstedt)), *T. pallidiceps* (Sjöstedt), *T. subcrenulatus* (Silvestri), *T. undulatus* (Fuller), *T. weissi* (Silvestri), *T. zavattarii* (Ghidini).

Etymology. From Latin *terni*, triple; *cubus*, cube; and *termes*, termite. Refers to *Cubitermes*-like species with triradial symmetry of the EVAs. Gender: masculine.

Comments. This genus corresponds to the clade V in this work and to the *muneris* and *bilobatodes* patterns in Josens & Deligne (2019).

Phylogenetic reconstruction of trait states

Ancestral reconstruction of traits was based on the three-gene dataset for Cubitermitinae (*i.e.* 31 species). Parsimony analyses indicated that 11 and 16 state shifts in worker EVA types and soldier labral lobes, respectively, were involved along the evolution of the *Cubitermes* complex. As detailed in the previous section, worker EVA types highly matched the phylogenetic relationships (Fig. 5 A); notably, sclerotized EVA spatulae appeared independently in *Polyspathotermes* and *Nititermes*. However, soldier labral lobes were found to be highly plastic and disappeared three times independently (Fig. 5 B; in *A. longiceps, Cr. albotarsalis*, and *Th. macrothorax*).

Discussion

Evolutionary trends in the Cubitermes *complex*

In the subfamily Cubitermitinae, the basic enteric valve is a funnel bearing six primary elongated prominent cushions alternating with non-prominent, secondary cushions (Noirot, 2001). The functioning of these enteric valves is still poorly understood. Globally, they act as filters, slowing down the fine soil particles and directing them towards the periphery of the second paunch (Bignell, 2000; Donovan, 2002). The EVAs are well developed in workers, which directly feed on crude soil. In the soldiers, they are either a little less developed than in workers or dramatically reduced, to the point of disappearing totally in the so-called ‘white-

gutted soldiers' (Scheffrahn *et al.*, 2017). In the imago caste, they are present but noticeably reduced (Josens & Deligne, 2019).

The ancestral EVA of Cubitermitinae matches well with Noirot's (2001) definition but has undergone various changes along the phylogeny: the subfamily Cubitermitinae is divided into three main clades (Bourguignon *et al.*, 2017), as follows: (*i*) the *Furculitermes* complex (*Furculitermes* and *Ophiotermes*) that has EVAs characterized by PCs not elongated but more or less shaped like dumbbells (see Sands, 1998; Fig. 2 L); the genus *Euchilotermes* has a similar digestive anatomy (Sands, 1998) and probably belongs in this clade as well; (*ii*) the *Basidentitermes* complex (five genera: *Basidentitermes, Noditermes, Orthotermes, Proboscitermes*, and *Procubitermes*) has maintained rather basic valves in workers (see Sands, 1998; Fig. 2 N), whereas soldiers are all white-gutted with vanishing EVA or no EVA at all (Scheffrahn *et al.*, 2017); some other genera (*Fastigitermes*, *Lepidotermes*, *Mucrotermes*, *Pilotermes*, *Profastigitermes*, *Unguitermes*, and *Unicornitermes*) also have white-gutted soldiers and might therefore join the *Basidentitermes* complex; and (*iii*) the *Cubitermes* complex (four genera in Bourguignon *et al.* (2017), now nine genera: *Apilitermes*, *Crenetermes*, *Cubitermes* (*sensu stricto*), *Isognathotermes*, *Megagnathotermes*, *Nitiditermes*, *Ternicubitermes*, *Polyspathotermes*, and *Thoracotermes*) that show various EVAs; the four remaining Cubitermitinae genera, with basic EVAs and dark-gutted soldiers (*Batillitermes*, *Okavangotermes*, *Ovambotermes*, and *Trapellitermes*; see Sands, 1998) might join the *Cubitermes* complex.

Enteric valve evolution (Fig. 5A)

Cubitermes (*sensu stricto* = the *bilobatus* pattern) is at the base of the *Cubitermes* complex; the species (of small size) remaining in this genus have small PCs with very few lateral supporting bristles and few distal strong setae (Fig. 2 A), and wide SCs. Their architecture is similar to the

ancestral EVA. Its sister species, *A. longiceps*, has also a basic EVA with clearly more lateral supporting bristles in accordance with its larger size (Fig. 2 J). *Cubitermes* and *A. longiceps* together make the sister clade to the other species of the *Cubitermes* complex.

Nititidermes diverges next and it is also the first with two spatulae, on PC3 and 4; moreover, PC1 is clearly longer and frequently also wider than the other PCs without spatulae, making the whole EVA asymmetrical. The SCs are as narrow as the PCs. This genus, however, unexpectedly merges the *sankurensis* pattern (with spatulae; Fig. 2 G) and the *oculatus* pattern (without spatulae; Fig. 2 F). Beside the absence of spatulae, the *oculatus* EVA looks like the *sankurensis* EVA; the similarity was strongly suggested by a long and wide PC1 and also by narrow SCs. *Nititidermes* therefore first evolved spatulae which were later lost in one lineage, probably rather recently in dry West African savannahs (Josens & Deligne, 2019). Although *Nititidermes berghei* could not be sequenced, it was incorporated into the *Cubitermes* complex (as expected by Sands, 1998) and now in the *sankurensis* pattern because of its bi-spatulated EVA. Unfortunately, *N. berghei* is only known from its type series collected near Lubumbashi, DRC. Another sample labelled *N. berghei* in the NHMUK collection, collected near Mbala, Zambia, clearly belongs to *N. orthognathus*.

The clade made by *Th. macrothorax* and *M. notandus* stemmed after *Nititidermes*, followed by *Ternicubitermes* and *Polyspathotermes*. *Thoracotermes macrothorax* displays a basic EVA (Fig. 2 O) whereas *M. notandus* developed long soft dorsal ridges and lateral comb-like supporting setae on every PC (Fig. 2 M); both have rather narrow SCs tending toward a spearhead shape.

Ternicubitermes merges the *muneris* and *bilobatodes* patterns (Fig. 2 B,C): their EVAs are aligned with the ancestral EVA; they are provided with more numerous and longer bristles in their downstream part than in *Cubitermes* species. They have triradial symmetry, the odd-numbered PCs being clearly longer than the even-numbered PCs. Both have wide SCs with

447 either homogeneous or tending toward a spearhead-shaped spine scattering. Grouping these two
448 patterns could be expected since several samples displayed intermediate EVAs.

449 *Polyspathotermes* is the second genus that developed spatulae, independently from
450 *Nititidermes*. This genus, however, merges the *sulcifrons* pattern (with six spatulae and
451 hexaradial EVA symmetry; Fig. 2 I) and the *oblectatus* pattern (three spatulae on PC 3-5, with
452 bilateral symmetry; Fig. 2 H). The latter shows unsclerotized sketches of spatulae on PC1, 2,
453 and 6. *Megagnathotermes katangensis* was transferred to *Polyspathotermes* because of its tri-
454 spatulated EVA (*oblectatus* pattern), a change confirmed by molecular data. However, the type
455 species *M. notandus* has distinctive EVA (Fig. 2 M) and sequences, which justify retaining
456 *Megagnathotermes* as a monospecific genus, close to *Thoracotermes*.

457 *Isognathotermes* and *Crenetermes* are among the last genera to appear in the *Cubitermes*
458 complex. *Isognathotermes* merges the *fungifaber* and *finitimus* patterns: their PCs differ from
459 the ancestral EVA by the presence of bristly crests or globular protrusions, respectively, on the
460 downstream part of the odd-numbered PCs (Fig. 2 D,E). If present on the even-numbered PCs,
461 those crests or globular protrusions are weakly developed; the EVAs therefore have triradial
462 symmetry. SCs are very wide with a homogeneous spine scattering. Merging these two patterns
463 could be expected since some samples showed intermediate EVAs. The sister genus
464 *Crenetermes*, as represented by *C. albotarsalis*, has tiny crests that are sketched on the odd-
465 numbered PCs (Fig. 2 K); it also has narrower SCs.

466

467 *Variation in Soldier labrum lobe*

468 The soldier's labrum (Fig. 5B) in *Cubitermes* (*sensu lato*) and *Megagnathotermes* is always
469 more or less deeply bifurcated, but this is not the case in other members of the *Cubitermes*
470 complex: *A. longiceps, Cr. albotarsalis*, and *Th. macrothorax* have not developed any lobe on
471 the labrum (Bouillon & Mathot, 1965). On the other hand, many genera of the *Furculitermes*

and *Basidentitermes* complexes (*Euchilotermes*, *Furculitermes*, *Mucrotermes*, *Noditermes*, *Ophiotermes*, *Pilotermes*, *Procubitermes*, and *Unguitermes*) also have soldiers with a bifurcated or at least indented labrum (Bouillon & Mathot, 1965). Moreover, the soldier's labrum is very flexible. Its precise shape can vary within a species and even within a single individual, the left lobe being different from the right one (pers. obs.).

Conclusions

This work provides valuable insights for the ongoing revision of *Cubitermes*. It is clear that the genus *Cubitermes sensu lato* is paraphyletic and required splitting into five monophyletic genera. The EVA of workers is the morphological trait best correlated with genetic data and is therefore the most efficient diagnostic trait. Along the *Cubitermes* complex phylogeny, sclerotized EVA spatulae appeared twice independently: as three or six spatulae in *Polyspathotermes* (*sulcifrons* and *oblectatus* patterns) and as two jaw-like spatulae in *Nitiditermes* (*sankurensis* pattern), which later disappeared in species with the *oculatus* pattern. Other morphological traits, mainly in soldiers, used in Sjöstedt's (1926) and Williams's (1966) keys (labrum shape, fore head projection, mandible curvature) are useful at the species level, but not genus. Our data confirm the hypothesis of Sands (1998), that the genera *Nitiditermes* and *Megagnathotermes* presents affinities to *Cubitermes*, and *M. notandus* remains the sole species of the latter genus. Further sequencing, especially of complete mitochondrial genomes (see Bourguignon *et al.*, 2017) or a multitude of orthologous genes generated by transcriptomic data (Bucek *et al.*, 2019) as well as the incorporation of more taxa, will enable to fully resolve the evolutionary history of the *Cubitermes* complex.

Acknowledgments

We are most grateful to our colleagues for the supply of *Cubitermes* samples from various African countries: Dr Pierre Akama (Université de Yaoundé 1, Cameroon), M Benoît Host (from Burundi), Patrick Kasangij (Université de Lubumbashi, DRC), Dr Carmel Kifukieto (Université de Kinshasa, DRC), Dr Laura Estelle Loko (Université Polytechnique d'Abomey, Benin), Dr Abdoulaye Baila Ndiaye (Université de Dakar, Senegal), Dr Saran Traoré (Université Polytechnique de Bobo, Burkina Faso), Mrs Geo Trembleau (from Gabon), and Dr Solange Makatia Wango (Université de Bangui, Central African Republic). We also acknowledge Dr Carmel Kifukieto for assistance during fieldwork in DRC, as well as Dr Tenon Coulibaly (Université Peleforo Gon Coulibaly, Côte d'Ivoire) and Dr Kanvaly Dosso (Université Nangui Abrogoua, Côte d'Ivoire) in Côte d'Ivoire; and Dr Thomas Bourguignon (Okinawa Institute of Science and Technology, Japan), Prof Rudolf Scheffrahn (University of Florida, Institute for Food and Agricultural Sciences, the USA), Dr Virginie Roy (Université Paris-Est Créteil, France) for providing samples of already published DNA sequences for re-examination. We are also grateful to Prof Rudolf Scheffrahn for providing us a photography of the enteric valve armature of the previously sequenced (accession KP026265) specimen 'CA1'. We would like to thank the museums that lent the material used in this work: the American Museum of Natural History (AMNH; New York, the United States of America), the Instituto di Entomologia Agraria dell'Università di Portici (IEAP; Napoli, Italy), the Museo Civico di Storia Naturale "Giacomo Doria" (MCGD; Genoa, Italy), the Natural History Museum (NHMUK; London, the United Kingdom), the Natuurhistorisch Museum of Maastricht (NHMM; Maastricht, the Netherlands), the Biosystematics Division of the Plant Protection Research Institute (PPRI; Pretoria, South Africa), and the Royal Museum for Central Africa (RMCA; Tervuren, Belgium). Finally, we are most grateful to two anonymous referees for their helpful comments on the manuscript.

This work was supported by grants from the Belgian National Fund for Scientific Research F.R.S.-FNRS (SH: PhD fellowship; YR: travel grant to Burundi, and grant PDR T.0065.15 to Côte d'Ivoire and Cameroon), a postdoctoral fellowship from the Japan Society for the Promotion of Science JSPS (to SH), and additional travel grants to YR from the Belgian Science Policy BELSPO (project COBIMFO; to DRC) and the DynAfFor project (Fonds Français pour l'Environnement FFEM and the Agence Française de Développement AFD; to Congo). The authors declare that there are no conflicts of interest.

Data Archiving

Sequences produced for this study have been deposited in GenBank under accessions MN646697 to MN646750 for *COI*, MN685897 to MN685956 for *COII*, and MN685957 to MN686017 for *28S rDNA* (see Supplementary Table S1 for details).

Supporting Information

Additional Supporting Information may be found in the online version of this manuscript.

Supplementary Methods SM-1: Molecular procedures used in this study.

Figure S1: Nuclear tree (**A**), cophyloplot (**B**), and total evidence tree (**C**) resulting from the StarBEAST2 three-genes analysis.

Figure S2: Mitochondrial (**A**) and nuclear (**B**) trees, cophyloplot (**C**), and total evidence tree (**D**) resulting from the StarBEAST2 two-gene analysis.

Table S1: Samples used in this study.

Table S2: Primers and cycling conditions used in this study.

Table S3: *COII* sequences retrieved from GenBank.

Table S4: List of valid names of the taxa formerly included (as in Krishna *et al.* 2013c) in the genera *Cubitermes*, *Megagnathotermes* and *Nititidermes*.

References

Bignell, D. E. (2000). Introduction to symbiosis. In 'Termites: Evolution, Sociality, Symbioses, Ecology'. (Eds T. Abe, D. E. Bignell, and M. Higashi.) pp. 189–208. (Kluwer Academic Publishers: Dordrecht, The Netherlands.). doi:10.1007/978-94-017-3223-9_9

Bouckaert, R., Heled, J., Kühnert, D., Vaughan, T., Wu, C. H., Xie, D., Suchard, M. A., Rambaut, A., and Drummond, A. J. (2014). BEAST 2: a software platform for bayesian evolutionary analysis. *PLoS Computational Biology* **10**, e1003537. doi:10.1371/journal.pcbi.1003537

Bouillon, A., and Mathot, G. (1965). Quel est ce termite africain? *Zooleo (Léopoldville)* **1**, 1–115.

Bouillon, A., and Vincke, P. P. (1971). Valvule entérique et révision du genre *Cubitermes* Wasmann. *Cubitermes bugeserae* sp. nov. (Isoptera, Termitidae). *Revue de Zoologie et de Botanique Africaines* **84**, 269–280.

Bourguignon, T., Lo, N., Cameron, S. L., Šobotník, J., Hayashi, Y., Shigenobu, S., Watanabe, D., Roisin, Y., Miura, T., and Evans, T. A. (2015). The evolutionary history of termites as inferred from 66 mitochondrial genomes. *Molecular Biology and Evolution* **32**, 406–421. doi:10.1093/molbev/msu308

Bourguignon, T., Lo, N., Šobotník, J., Ho, S. Y. W., Iqbal, N., Coissac, É., Lee, M., Jendryka, M. M., Sillam-Dussès, D., Křížková, B., Roisin, Y., and Evans, T. A. (2017). Mitochondrial phylogenomics resolves the global spread of higher termites, ecosystem engineers of the tropics. *Molecular Biology and Evolution* **34**, 589–597. doi:10.1093/molbev/msw253

Bucek, A., Šobotník, J., He, S., Shi, M., McMahon, D. P., Holmes, E. C., Roisin, Y., Lo, N., and Bourguignon, T. (2019). Evolution of termite symbiosis informed by transcriptome-based phylogenies. *Current Biology* **29**, 3728-3734.e4. doi:10.1016/j.cub.2019.08.076

Darriba, D., Taboada, G. L., Doallo, R., and Posada, D. (2012). jModelTest 2: more models, new heuristics and parallel computing. *Nature Methods* **9**, 772. doi:10.1038/nmeth.2109

Donovan, S. E. (2002). A morphological study of the enteric valves of the Afrotropical Apicotermitinae (Isoptera: Termitidae). *Journal of Natural History* **36**, 1823–1840. doi:10.1080/00222930110062309

Donovan, S. E., Eggleton, P., and Bignell, D. E. (2001a). Gut content analysis and a new feeding group classification of termites. *Ecological Entomology* **26**, 356–366. doi:10.1046/j.1365-2311.2001.00342.x

Donovan, S. E., Eggleton, P., Dubbin, W. E., Batchelder, M., and Dibog, L. (2001b). The effect of a soil-feeding termite, *Cubitermes fungifaber* (Isoptera: Termitidae) on soil properties: termites may be an important source of soil microhabitat heterogeneity in tropical forests. *Pedobiologia* **45**, 1–11. doi:10.1078/0031-4056-00063

Dray, S., and Dufour, A. B. (2007). The ade4 package: implementing the duality diagram for ecologists. *Journal of Statistical Software* **22**, 1–20. doi:10.1.1.177.8850

Edgar, R. C. (2004). MUSCLE: a multiple sequence alignment method with reduced time and space complexity. *BMC Bioinformatics* **5**, 1–19. doi:10.1186/1471-2105-5-113

Emerson, A. E. (1960). Six new genera of Termitinae from the Belgian Congo (Isoptera, Termitidae). *American Museum Novitates* **1988**, 1–49.

Engel, M. S., Grimaldi, D. A., and Krishna, K. (2009). Termites (Isoptera): their phylogeny, classification, and rise to ecological dominance. *American Museum Novitates* **3650**, 1–27.

Haviland, G. D. (1898). Observations on termites; with descriptions of new species. *Journal of the Linnean Society of London, Zoology* **26**, 358–442, pl. 22–25.

Hijmans, R. J. (2019). geosphere: spherical trigonometry. Version 1.5-10. Available at: https://cran.r-project.org/package=geosphere

Inward, D. J. G., Vogler, A. P., and Eggleton, P. (2007). A comprehensive phylogenetic analysis of termites (Isoptera) illuminates key aspects of their evolutionary biology. *Molecular Phylogenetics and Evolution* **44**, 953–967. doi:10.1016/j.ympev.2007.05.014

Josens, G., and Deligne, J. (2019). Species groups in the genus *Cubitermes* (Isoptera: Termitidae) defined on the basis of enteric valve morphology. *European Journal of Taxonomy*, 1–72. doi:10.5852/ejt.2019.515

Josens, G., and Wango, S. P. M. (2019). Niche differentiation between two sympatric *Cubitermes* species (Isoptera, Termitidae, Cubitermitinae) revealed by stable C and N isotopes. *Insects* **10**, 38. doi:10.3390/insects10020038

Kimura, M. (1980). A simple method for estimating evolutionary rate of base substitutions through comparative studies of nucleotide sequences. *Journal of Molecular Evolution* **16**, 111–120. doi:10.1007/BF01731581

Krishna, K., Grimaldi, D. A., Krishna, V., and Engel, M. S. (2013a). Treatise on the Isoptera of the World. 1. Introduction. *Bulletin of the American Museum of Natural History* **377**, 1–200. doi:10.1206/377.1

Krishna, K., Grimaldi, D. A., Krishna, V., and Engel, M. S. (2013b). Treatise on the Isoptera of the World. 4. Termitidae (Part One). *Bulletin of the American Museum of Natural History* **377**, 973–1494. doi:10.1206/377.4

Krishna, K., Grimaldi, D. A., Krishna, V., and Engel, M. S. (2013c). Treatise on the Isoptera of the World. 5. Termitidae (Part Two). *Bulletin of the American Museum of Natural History* **377**, 1495–1988. doi:10.1206/377.5

Kumar, S., Stecher, G., Li, M., Knyaz, C., and Tamura, K. (2018). MEGA X: molecular evolutionary genetics analysis across computing platforms. *Molecular Biology and Evolution* **35**, 1547–1549. doi:10.1093/molbev/msy096

Maddison, W. P., and Maddison, D. R. (2019). Mesquite: a modular system for evolutionary analysis. Version 3.6. Available at: http://mesquiteproject.org

Mantel, N. (1967). The detection of disease clustering and a generalized regression approach. *Cancer Research* **27**, 209–220.

Noirot, C. (2001). The gut of termites (Isoptera): comparative anatomy, systematics, phylogeny. II. - Higher termites (Termitidae). *Annales de la Société Entomologique de France (Nouvelle Série)* **37**, 431–471.

Ogilvie, H. A., Bouckaert, R. R., and Drummond, A. J. (2017). StarBEAST2 brings faster species tree inference and accurate estimates of substitution rates. *Molecular Biology and Evolution* **34**, 2101–2114. doi:10.1093/molbev/msx126

Okwakol, M. J. N. (1987). Effects of *Cubitermes testaceus* (Williams) on some physical and chemical properties of soil in a grassland area of Uganda. *African Journal of Ecology* **25**, 147–153. doi:10.1111/j.1365-2028.1987.tb01101.x

Paradis, E., Claude, J., and Strimmer, K. (2004). APE: analyses of phylogenetics and evolution in R language. *Bioinformatics* **20**, 289–290. doi:10.1093/bioinformatics/btg412

R Development Core Team (2018). R: A Language and Environment for Statistical Computing.

Rambaut, A. (2017). FigTree v1.4.3. Available at: https://github.com/rambaut/figtree/releases

Rambaut, A., Suchard, M., Xie, W., and Drummond, A. J. (2014). Tracer v1.6.

Ronquist, F., Teslenko, M., van der Mark, P., Ayres, D. L., Darling, A., Höhna, S., Larget, B., Liu, L., Suchard, M. A., and Huelsenbeck, J. P. (2012). MrBayes 3.2: Efficient Bayesian phylogenetic inference and model choice across a large model space. *Systematic Biology* **61**, 539–542. doi:10.1093/sysbio/sys029

Roy, V., Demanche, C., Livet, A., and Harry, M. (2006). Genetic differentiation in the soil-feeding termite *Cubitermes* sp. *affinis subarquatus*: occurrence of cryptic species revealed by nuclear and mitochondrial markers. *BMC Evolutionary Biology* **6**, 102. doi:10.1186/1471-2148-6-102

Ruelle, J. E. (1975). Type specimens of Isoptera in the National Collection of Insects, Pretoria. *Entomology Memoir, Department of Agricultural and Technical Services, Republic of South Africa* **45**, 1–22.

Sands, W. A. (1998). 'The identification of worker castes of termite genera from soils of Africa and the Middle East'. (CABI Publishing.)

Sands, W. A. (1972). The soldierless termites of Africa (Isoptera, Termitidae). *Bulletin of the British Museum (Natural History) Entomology* Supplement **18**, 1–244.

Scheffrahn, R. H., Bourguignon, T., Bordereau, C., Hernandez-Aguilar, R. A., Oelze, V. M., Dieguez, P., Šobotnik, J., and Pascual-Garrido, A. (2017). White-gutted soldiers: simplification of the digestive tube for a non-particulate diet in higher Old World termites (Isoptera: Termitidae). *Insectes Sociaux* **64**, 525–533. doi:10.1007/s00040-017-0572-9

Silvestri, F. (1912). Termiti raccolte da L. Fea alla Guinea Portoghese e alle isole S. Thomè, Annobon, Principe e Fernando Poo. *Annali del Museo Civico di Storia Naturale di Genova (Ser. 3)* **5**, 211–255.

Sjöstedt, Y. (1913). Über Termiten aus dem inneren Kongo, Rhodesia, und Deutsch-Ostafrika. *Revue Zoologique Africaine (Bruxelles)* **2**, 354–391, pl. VIII–X.

Sjöstedt, Y. (1926). Revision der Termiten Afrikas. 3. Monographie. *Kungliga Svenska Vetenskapsakademiens Handlingar (3)* **3**, 1–419, 16pl.

Snyder, T. E. (1949). Catalog of the Termites (Isoptera) of the World. *Smithsonian Miscellaneous Collections* **112**, 1–490.

Vincenty, T. (1975). Direct and inverse solutions of geodesics on ellipsoid with applications of nested equations. *Survey Review* **23**, 88–93.

Wango, S. P., and Josens, G. (2011). Comparison of nest shapes and densities of two sympatric species of *Cubitermes* (Isoptera: Termitidae: Termitinae) as clues for the study of their population dynamics. *African Zoology* **46**, 156–168. doi:10.3377/004.046.0106

Wasmann, E. (1906). Beispiele rezenter artenbildung bei ameisengästen und termitengästen. *Biologisches Centralblatt* **26**, 565–580.

Wasmann, S. J. (1911). Zur Kenntnis der Termiten und Termitengäste von Belgischen Congo (Schluss, mit 2 Tafeln.). *Revue Zoologique Africaine (Bruxelles)* **1**, 145–176.

Williams, R. M. C. (1966). The East African termites of the genus *Cubitermes* (Isoptera: Termitidae). *Transactions of the Royal Entomological Society of London* **118**, 73–118.

Wood, T. G., Johnson, R. A., and Anderson, J. M. (1983). Modification of soils in Nigerian savanna by soil-feeding *Cubitermes* (Isoptera, termitidae). *Soil Biology and Biochemistry* **15**, 575–579. doi:10.1016/0038-0717(83)90052-4

679 **Figure captions**

680 **Fig. 1.** Pictures of (**A**) living soldier and workers of *Isognathotermes planifrons*
681 (Sjöstedt) (Cameroon; scale bar, 0.5 cm), young (**B**) and old (**C**) nests of *Isognathotermes*
682 *severus* (Silvestri) (Central African Republic; scale bars, 10 cm), and (**D**) landscape
683 characterized by mounds of *Nititidermes* sp. NS22 (Côte d'Ivoire). Credits: Y. Roisin (A, D),
684 and G. Josens (B, C). This figure is available in colour in the online version.

685 **Fig. 2.** Enteric valve armature patterns from workers of studied taxa (described in Table 1): (**A**)
686 *Cubitermes exiguus* Mathot; (**B**) *Ternicubitermes weissi* (Silvestri); (**C**) *Ternicubitermes*
687 *muneris* (Sjöstedt); (**D**) *Isognathotermes fungifaber* (Sjöstedt); (**E**) *Isognathotermes finitimus*
688 (Schmitz); (**F**) *Nititidermes oculatus* (Silvestri); (**G**) *Nititidermes sankurensis* (Wasmann); (**H**)
689 *Polyspathotermes oblectatus* (Harris); (**I**) *Polyspathotermes sulcifrons* (Wasmann); (**J**)
690 *Apilitermes longiceps* (Sjöstedt); (**K**) *Crenetermes albotarsalis* (Sjöstedt); (**L**) *Furculitermes*
691 *parviceps* Emerson; (**M**) *Megagnathotermes notandus* Silvestri; (**N**) *Procubitermes aburiensis*
692 Sjöstedt; (**O**) *Thoracotermes macrothorax* (Sjöstedt). Scale bars, 0.5 mm. This figure is
693 available in colour in the online version.

694 **Fig. 3.** Maximum clade credibility ultrametric mitochondrial (linked *COI* and *COII*) tree
695 resulting from Bayesian inference using the StarBEAST2 method on the three-gene dataset (for
696 the nuclear tree, cophyloplot and total evidence trees, see Supplementary Fig. S1). Node support
697 values are Bayesian posterior probabilities (BPP). Scale bar indicates the mean number of
698 substitutions per site. Genera which previously made *Cubitermes* Wasmann paraphyletic are
699 indicated in bold.

700 **Fig. 4.** Non-ultrametric 50% majority rule consensus Bayesian phylogenetic tree generated by
701 MrBayes using the *COII* alignment of sequences produced in this study and retrieved from
702 GenBank (for details, see Tables S1 and S3). Node support values are Bayesian posterior
703 probabilities (BPP). Scale bar indicates the mean number of substitutions per site. Genera which
704 previously made *Cubitermes* Wasmann paraphyletic are indicated in bold.

705 **Fig. 5.** Ancestral reconstruction of (**A**) workers' EVA types (see Table 1 A), and (**B**) soldiers'
706 labral lobes (Absence of lobes; Digitiform; Subtruncated; Truncated; Triangular), on the
707 mitochondrial (*COI* and *COII*) BI tree. Ancestral states were reconstructed using Mesquite v3.6
708 under a parsimony model with unordered characters for each trait. Genera which previously
709 made *Cubitermes* Wasmann paraphyletic are indicated in bold. This figure is available in colour
710 in the online version.

Table 1: Overview of enteric valve armatures (EVAs) among (**A**) groups of species described within the genus *Cubitermes* (*sensu lato*) and derived monophyletic genera, as well as (**B**) non *Cubitermes* species, with details on primary cushions (PCs) and secondary cushions (SCs). Asterisks denote observations made on two to seven individuals. In (**A**), the last three columns refer to genus assignment based on molecular data (see Results).

	EVA type	Valve symmetry	PCs			SCs	Comments	Genus revision (genetic clade) Type species
			Shape (pairs of supporting bristles)	Sclerotized spatulae	Crests	Size and spine scattering		
(A) *Cubitermes* species (*sensu lato*)	*bilobatus* See Fig. 2 A	triradial to bilateral	nearly triangular (2-6)	none	none	wider than PCs; generally heterogeneous		***Cubitermes*** **Wasmann, 1906: 573 (clade I)** *Termes bilobatus* Haviland, 1898: 411-412
	bilobatodes See Fig. 2 B	triradial	fusiform (10-30)	none	none	wider than PCs; spearhead shaped	sometimes intermediate with *sulcifrons* EVA	***Ternicubitermes*** **Josens & Deligne gen.n. (clade V)** *Cubitermes bilobatodes* Silvestri, 1912: 247-249
	muneris See Fig. 2 C	triradial	roughly rectangular (10-19)	none	none	wider than PCs; homogeneous	sometimes intermediate with *bilobatodes* EVA	
	fungifaber See Fig. 2 D	triradial	triangular or fusiform (13-30)	none	high, on PC1, 3 & 5	wider than PCs; homogeneous	sometimes intermediate with *finitimus* EVA	***Isognathotermes*** **Sjöstedt, 1926: 216 (clade III)** *Eutermes* (*Cubitermes*) *minitabundus* Sjöstedt, 1913: 368-369
	finitimus See Fig. 2 E	triradial	roughly rectangular (17-37)	none	wide, on PC1, 3 & 5	wider than PCs; homogeneous	sometimes intermediate with *fungifaber* EVA	
	oculatus See Fig. 2 F	bilateral	nearly triangular (3-8)	none	none	not wider than PCs; SCs surrounding PC1 faint or lacking		***Nititermes*** **Emerson, 1960: 3-10 (clade II)** *Nititermes berghei* Emerson, 1960: 10-12
	sankurensis See Fig. 2 G	none	roughly triangular (8-24)	2 (PC3 & 4)	none	not wider than 120% of PCs; SCs surrounding PC1 weakly developed		
	oblectatus See Fig. 2 H	bilateral	roughly rectangular to fusiform (14-23)	3 (PC3, 4 & 5)	high, on PC1, 3 & 5	2-3 times wider than PCs; homogeneous	spatulae sketched on PC1, 2 & 6, not sclerotized	***Polyspathotermes*** **Josens & Deligne gen.n. (clade IV)** *Cubitermes sulcifrons* Wasmann, 1911: 156-158
	sulcifrons See Fig. 2 I	hexaradial	more or less fusiform (13-23)	6 (all PCs)	high, on all PCs	spearhead shaped or wider than PCs and homogeneous		

717 **Table 1. Continued (B).**

	EVA type	Valve symmetry	PCs: Shape (pairs of supporting bristles)	PCs: Sclerotized spatulae	PCs: Crests	SCs: Size and spine scattering	Comments	Genus
(B) Other Cubitermitinae species	*Apilitermes longiceps* (Sjöstedt) * See Fig. 2 J	hexaradial to triradial	nearly triangular (15-18)	none	none	as wide as PCs; homogeneous or spearhead shaped		***Apilitermes*** **Holmgren**
	Crenetermes albotarsalis (Sjöstedt) * See Fig. 2 K	triradial	nearly triangular to fusiform (15-18)	none	on PC1, 3 & 5	as wide as PCs; homogeneous	hairy appearance	***Crenetermes*** **Silvestri**
	Furculitermes parviceps Emerson * See Fig. 2 L	triradial to bilateral	asymmetric dumbbell shaped (10-15)	none	none	as wide as PCs; homogeneous	hairy oval SCs	***Furculitermes*** **Emerson**
	Megagnathotermes notandus Silvestri* See Fig. 2 M	triradial	nearly triangular plus fusiform pectinate sides (16-19)	none	long, on all PCs	not wider than PCs; tendency towards two groups	comb-like supporting bristles	***Megagnathotermes*** **Silvestri**
	Procubitermes aburiensis Sjöstedt * See Fig. 2 N	triradial	nearly triangular to fusiform (17-20)	none	none	not wider than PCs; tendency towards spearhead shaped	close to *bilobatodes* EVA but with narrow SCs	***Procubitermes*** **Silvestri**
	Thoracotermes macrothorax (Sjöstedt) * See Fig. 2 O	hexaradial	nearly triangular (17-23)	none	none	not wider than PCs; tendency towards two groups		***Thoracotermes*** **Wasmann**

718

FIGURE 1.

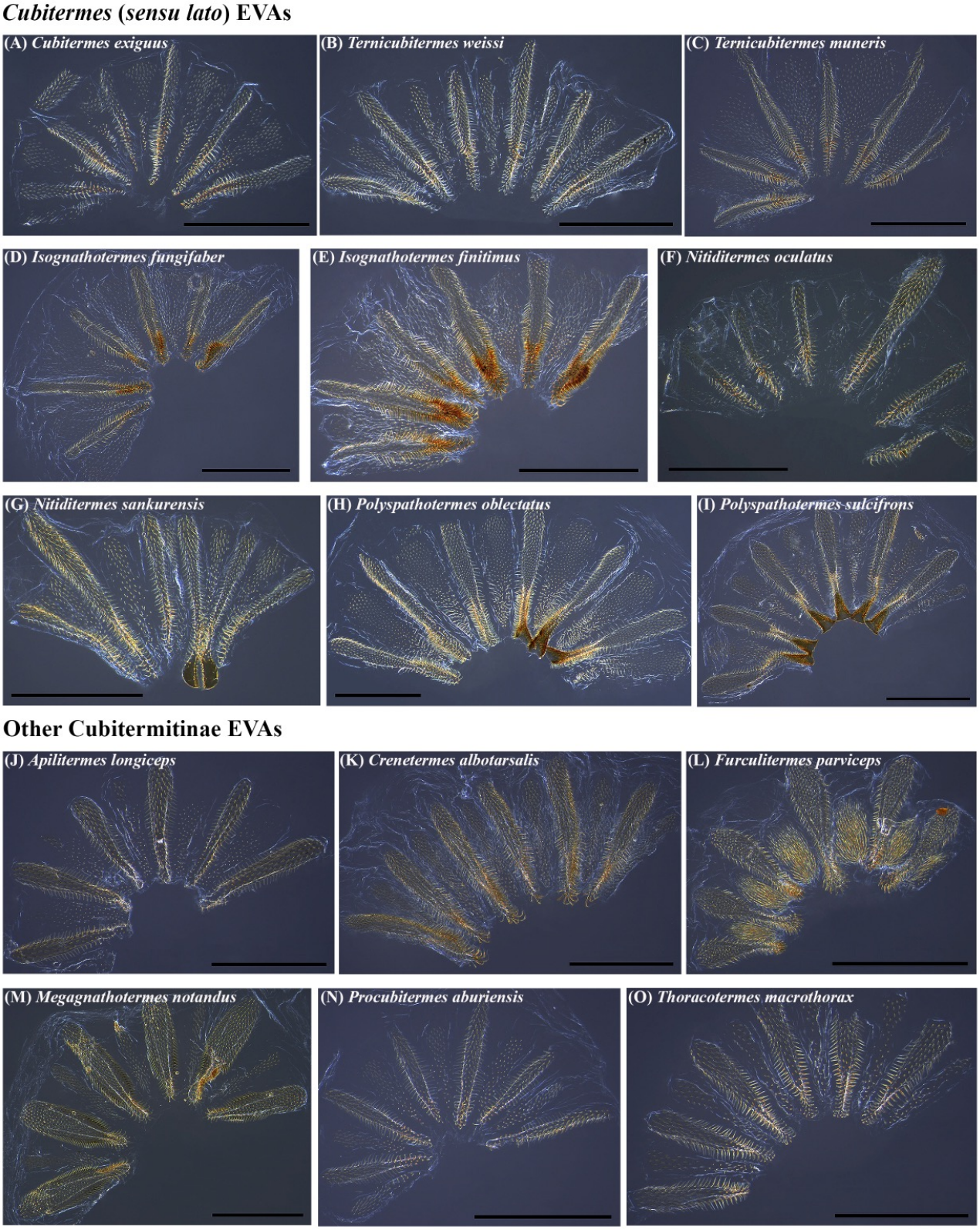
Cubitermes (*sensu lato*) EVAs
(A) *Cubitermes exiguus*
(B) *Ternicubitermes weissi*
(C) *Ternicubitermes muneris*
(D) *Isognathotermes fungifaber*
(E) *Isognathotermes finitimus*
(F) *Nitiditermes oculatus*
(G) *Nitiditermes sankurensis*
(H) *Polyspathotermes oblectatus*
(I) *Polyspathotermes sulcifrons*
Other Cubitermitinae EVAs
(J) *Apilitermes longiceps*
(K) *Crenetermes albotarsalis*
(L) *Furculitermes parviceps*
(M) *Megagnathotermes notandus*
(N) *Procubitermes aburiensis*
(O) *Thoracotermes macrothorax*

FIGURE 2.

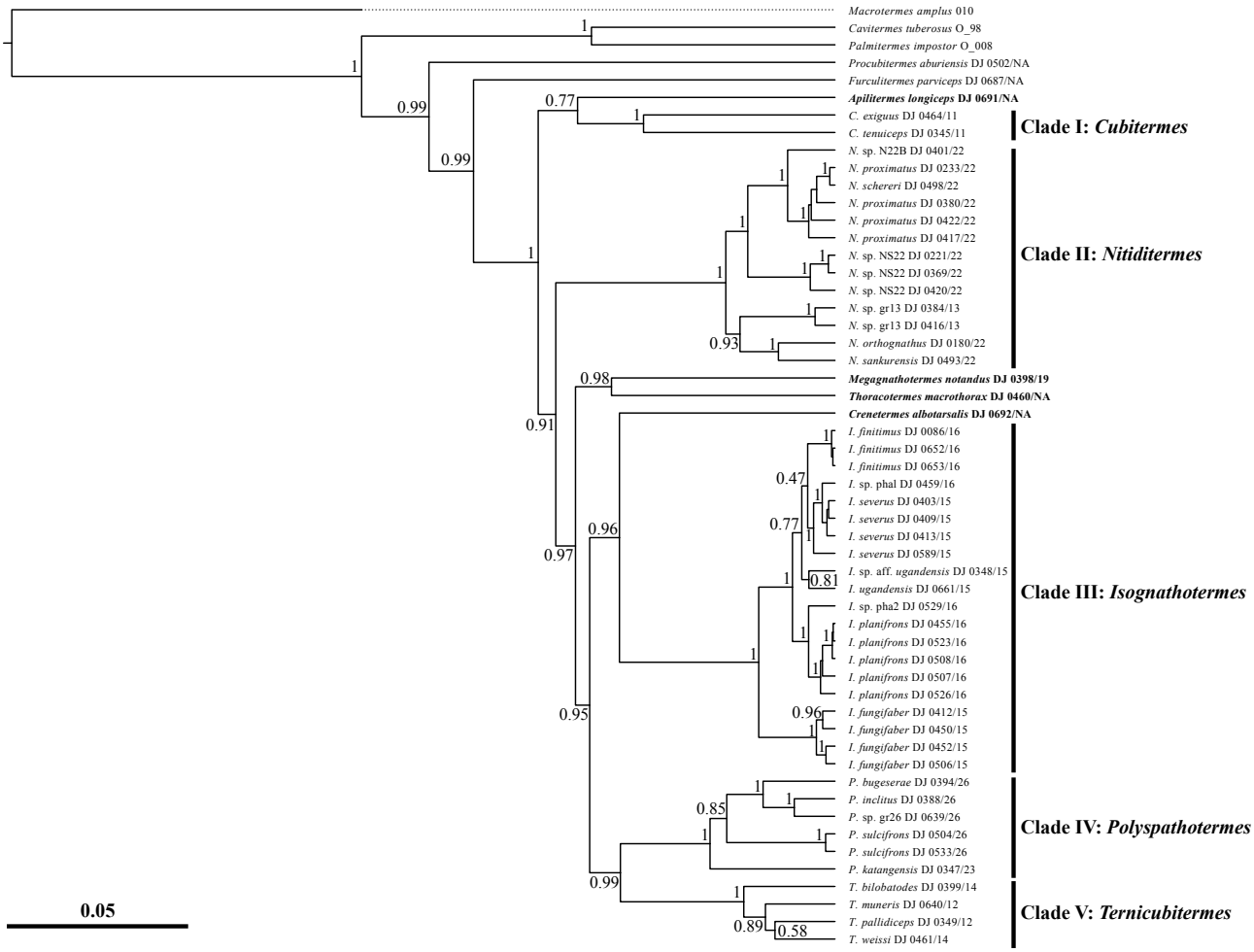

723

724 **FIGURE 3.**

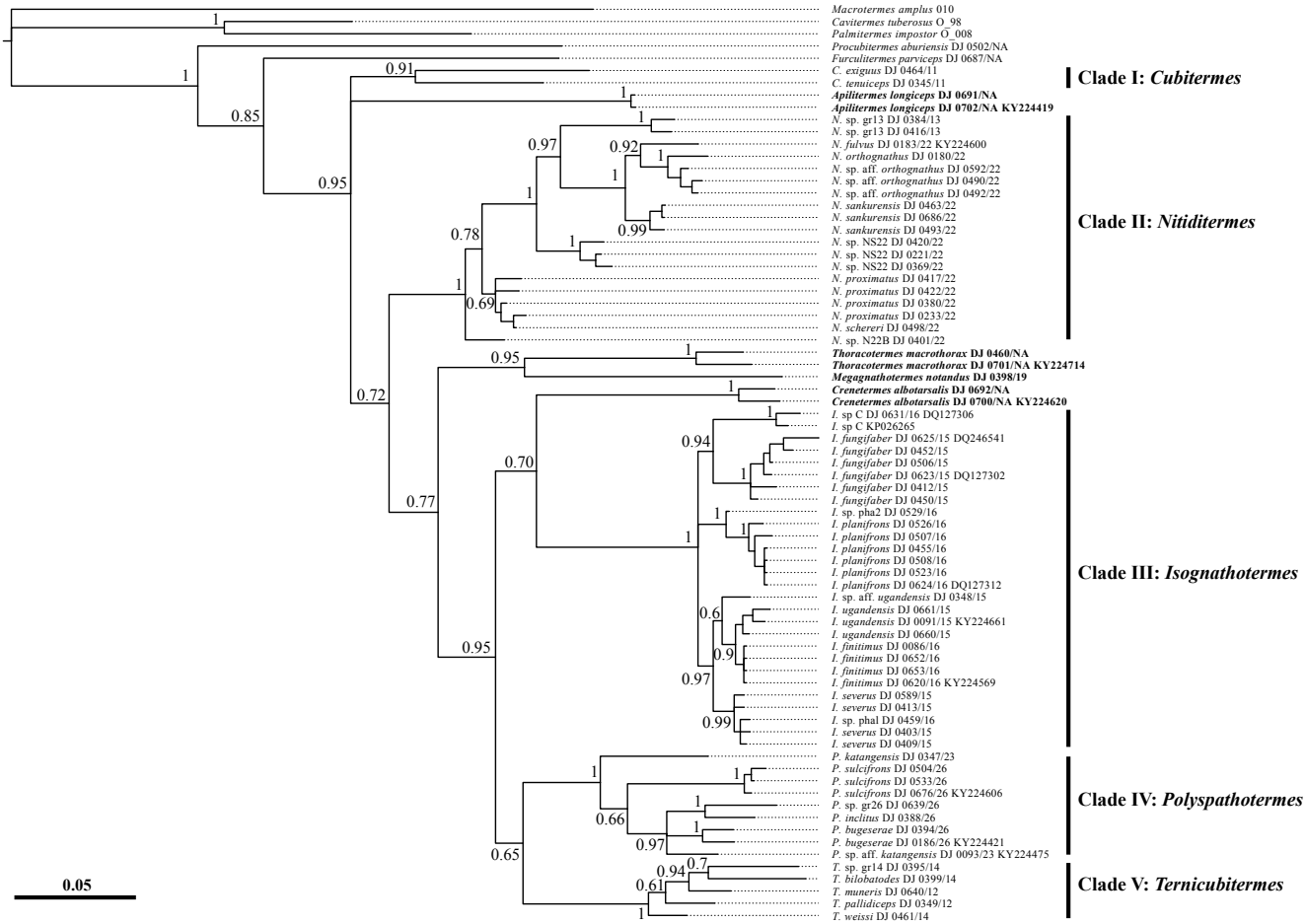
Macrotermes amplus 010
Cavitermes tuberosus O_98
Palmitermes impostor O_008
Procubitermes aburiensis DJ 0502/NA
Furculitermes parviceps DJ 0687/NA
C. exiguus DJ 0464/11
C. tenuiceps DJ 0345/11
Apilitermes longiceps DJ 0691/NA
Apilitermes longiceps DJ 0702/NA KY224419
N. sp. gr13 DJ 0384/13
N. sp. gr13 DJ 0416/13
N. fulvus DJ 0183/22 KY224600
N. orthognathus DJ 0180/22
N. sp. aff. orthognathus DJ 0592/22
N. sp. aff. orthognathus DJ 0490/22
N. sp. aff. orthognathus DJ 0492/22
N. sankurensis DJ 0463/22
N. sankurensis DJ 0686/22
N. sankurensis DJ 0493/22
N. sp. NS22 DJ 0420/22
N. sp. NS22 DJ 0221/22
N. sp. NS22 DJ 0369/22
N. proximatus DJ 0417/22
N. proximatus DJ 0422/22
N. proximatus DJ 0380/22
N. proximatus DJ 0233/22
N. schereri DJ 0498/22
N. sp. N22B DJ 0401/22
Thoracotermes macrothorax DJ 0460/NA
Thoracotermes macrothorax DJ 0701/NA KY224714
Megagnathotermes notandus DJ 0398/19
Crenetermes albotarsalis DJ 0692/NA
Crenetermes albotarsalis DJ 0700/NA KY224620
I. sp C DJ 0631/16 DQ127306
I. sp C KP026265
I. fungifaber DJ 0625/15 DQ246541
I. fungifaber DJ 0452/15
I. fungifaber DJ 0506/15
I. fungifaber DJ 0623/15 DQ127302
I. fungifaber DJ 0412/15
I. fungifaber DJ 0450/15
I. sp. pha2 DJ 0529/16
I. planifrons DJ 0526/16
I. planifrons DJ 0507/16
I. planifrons DJ 0455/16
I. planifrons DJ 0508/16
I. planifrons DJ 0523/16
I. planifrons DJ 0624/16 DQ127312
I. sp. aff. ugandensis DJ 0348/15
I. ugandensis DJ 0661/15
I. ugandensis DJ 0091/15 KY224661
I. ugandensis DJ 0660/15
I. finitimus DJ 0086/16
I. finitimus DJ 0652/16
I. finitimus DJ 0653/16
I. finitimus DJ 0620/16 KY224569
I. severus DJ 0589/15
I. severus DJ 0413/15
I. sp. phal DJ 0459/16
I. severus DJ 0403/15
I. severus DJ 0409/15
P. katangensis DJ 0347/23
P. sulcifrons DJ 0504/26
P. sulcifrons DJ 0533/26
P. sulcifrons DJ 0676/26 KY224606
P. sp. gr26 DJ 0639/26
P. inclitus DJ 0388/26
P. bugeserae DJ 0394/26
P. bugeserae DJ 0186/26 KY224421
P. sp. aff. katangensis DJ 0093/23 KY224475
T. sp. gr14 DJ 0395/14
T. bilobatodes DJ 0399/14
T. muneris DJ 0640/12
T. pallidiceps DJ 0349/12
T. weissi DJ 0461/14
Clade I: Cubitermes
Clade II: Nititidermes
Clade III: Isognathotermes
Clade IV: Polyspathotermes
Clade V: Ternicubitermes
0.05

FIGURE 4.

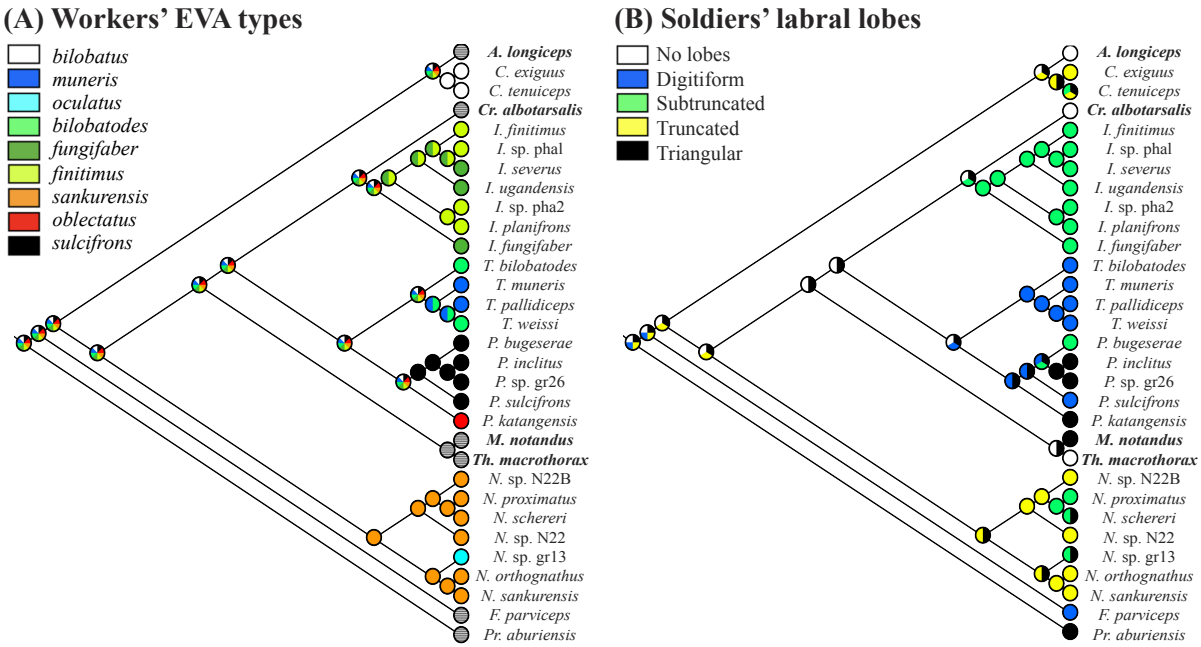
(A) Workers' EVA types
bilobatus
muneris
oculatus
bilobatodes
fungifaber
finitimus
sankurensis
oblectatus
sulcifrons
A. longiceps
C. exiguus
C. tenuiceps
Cr. albotarsalis
I. finitimus
I. sp. phal
I. severus
I. ugandensis
I. sp. pha2
I. planifrons
I. fungifaber
T. bilobatodes
T. muneris
T. pallidiceps
T. weissi
P. bugeserae
P. inclitus
P. sp. gr26
P. sulcifrons
P. katangensis
M. notandus
Th. macrothorax
N. sp. N22B
N. proximatus
N. schereri
N. sp. N22
N. sp. gr13
N. orthognathus
N. sankurensis
F. parviceps
Pr. aburiensis
(B) Soldiers' labral lobes
No lobes
Digitiform
Subtruncated
Truncated
Triangular
A. longiceps
C. exiguus
C. tenuiceps
Cr. albotarsalis
I. finitimus
I. sp. phal
I. severus
I. ugandensis
I. sp. pha2
I. planifrons
I. fungifaber
T. bilobatodes
T. muneris
T. pallidiceps
T. weissi
P. bugeserae
P. inclitus
P. sp. gr26
P. sulcifrons
P. katangensis
M. notandus
Th. macrothorax
N. sp. N22B
N. proximatus
N. schereri
N. sp. N22
N. sp. gr13
N. orthognathus
N. sankurensis
F. parviceps
Pr. aburiensis

FIGURE 5.

ELECTRONIC SUPPLEMENTARY MATERIALS

Phylogeny and revision of the '*Cubitermes* complex' termites (Termitidae: Cubitermitinae)

Simon Hellemans[1,2,*], Jean Deligne[3,4], Yves Roisin[2], Guy Josens[3]

[1]Okinawa Institute of Science & Technology Graduate University, 1919-1 Tancha, Onna-son, Okinawa 904-0495, Japan.

[2]Evolutionary Biology & Ecology, Université Libre de Bruxelles, Avenue F.D. Roosevelt 50, CP 160/12, B-1050 Brussels, Belgium.

[3]Laboratoire d'Écologie Végétale et Biogéochimie, Université Libre de Bruxelles, Avenue F.D. Roosevelt 50, CP 244, B-1050 Brussels, Belgium.

[4]Royal Museum for Central Africa, Entomology, Leuvensesteenweg 13, 3080 Tervuren, Belgium.

*Corresponding author: simon.hellemans@gmail.com

A. Supplementary Figures

(S1A) Three-gene analysis: nuclear tree (*28S rDNA*)

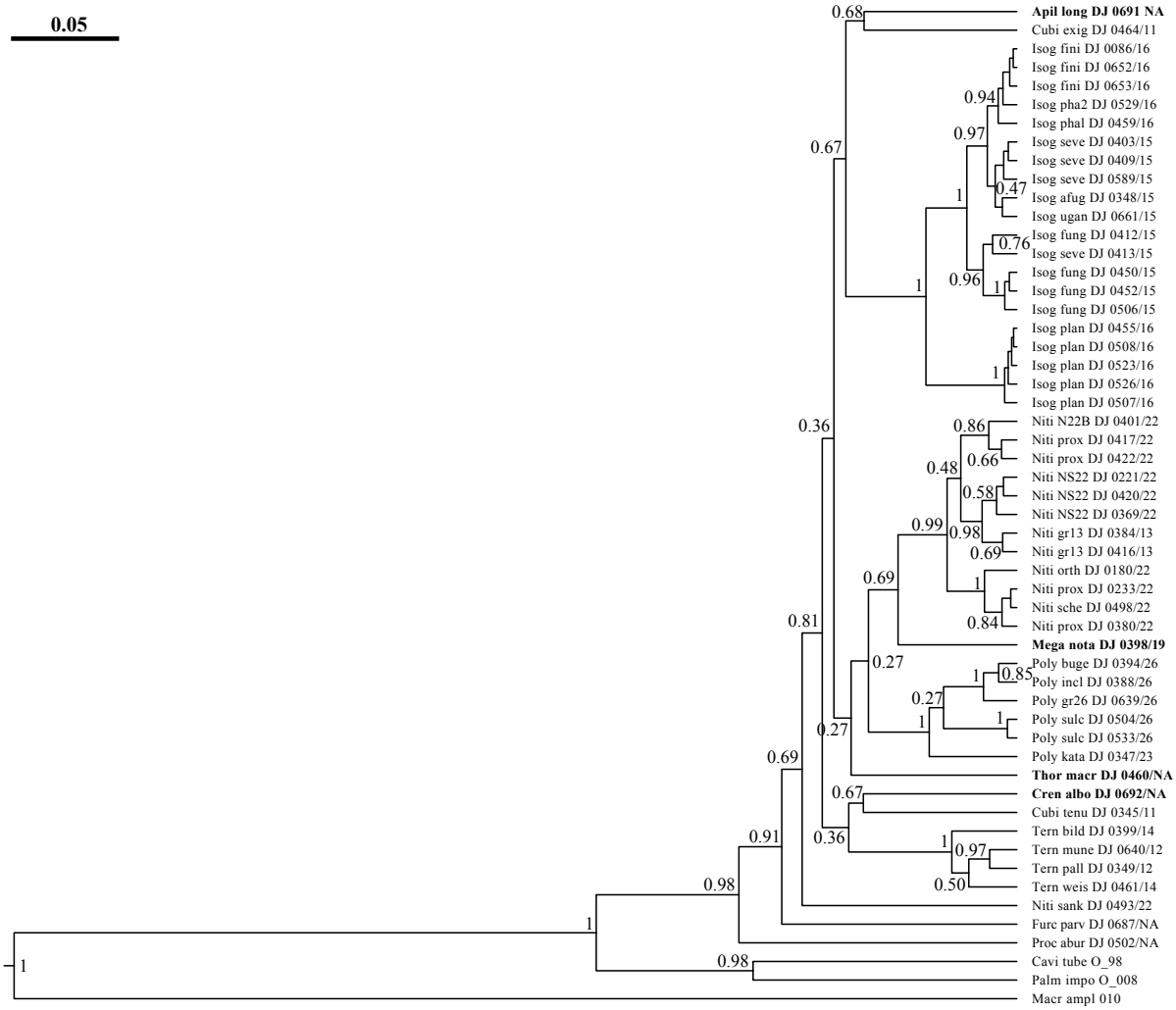

(S1B) Three-gene analysis: cophyloplot

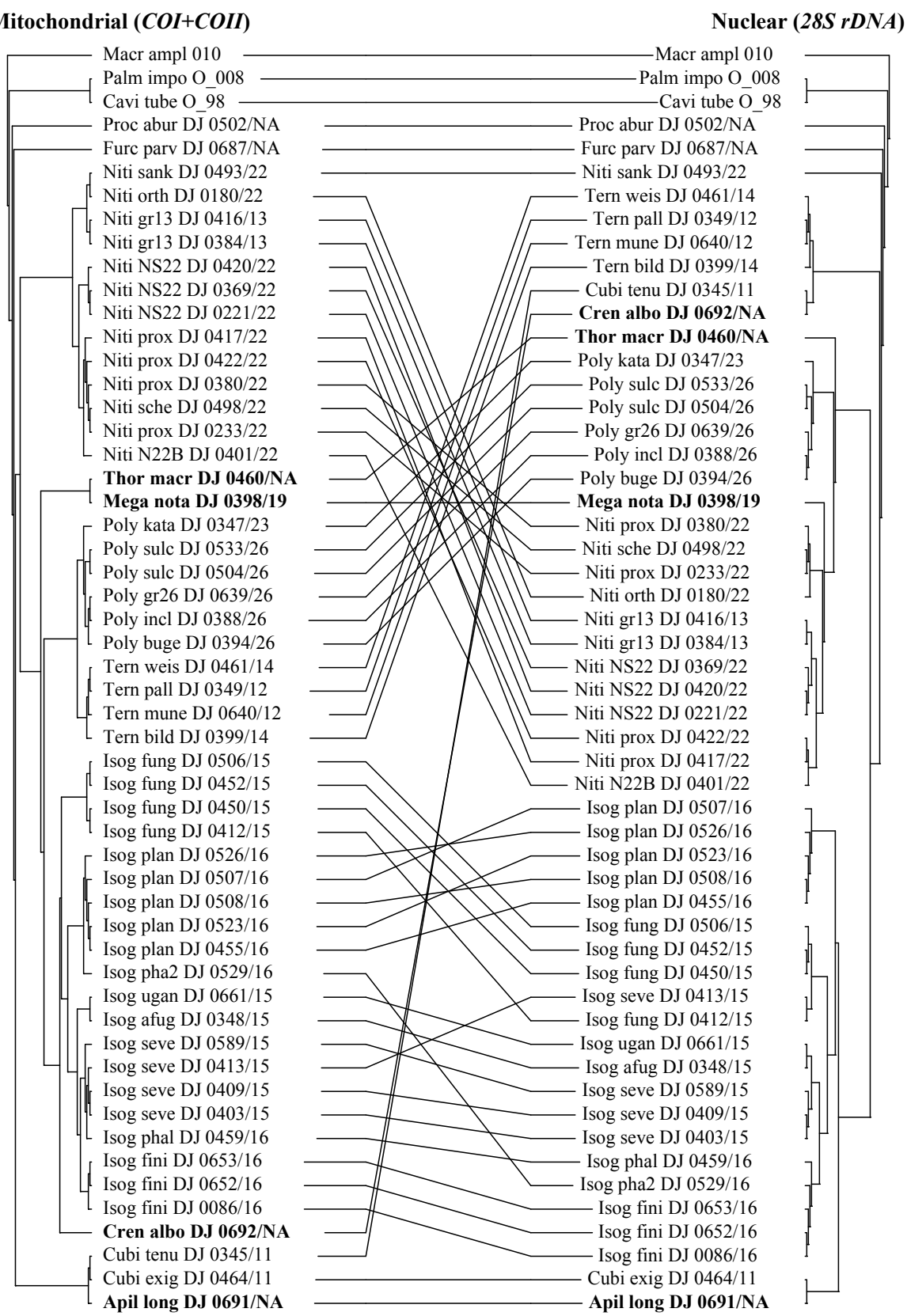

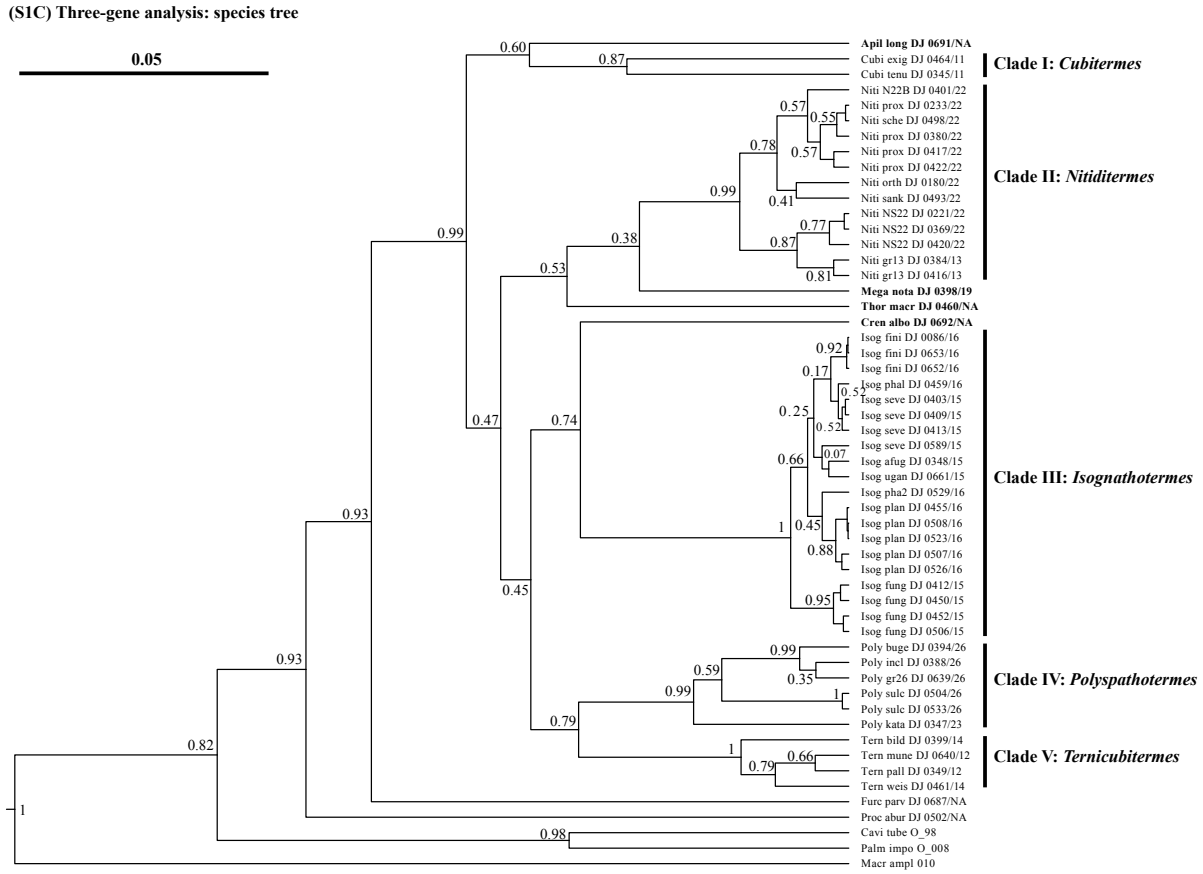

Fig. S1. Maximum clade credibility ultrametric gene and species trees resulting from Bayesian inference using the StarBEAST2 method for the three-gene dataset (mitochondrial linked *COI+COII* and nuclear *28S rDNA*; 54 sequences): (**A**) nuclear tree, (**B**) a cophyloplot showing the incongruence between the mitochondrial and nuclear trees, and (**C**) the total evidence tree. Node support values are Bayesian posterior probabilities (BPP). Scale bar indicates the mean number of substitutions per site. Genera which previously made *Cubitermes* paraphyletic are indicated in bold.

(S2A) Two-gene analysis: mitochondrial tree (*COII*)

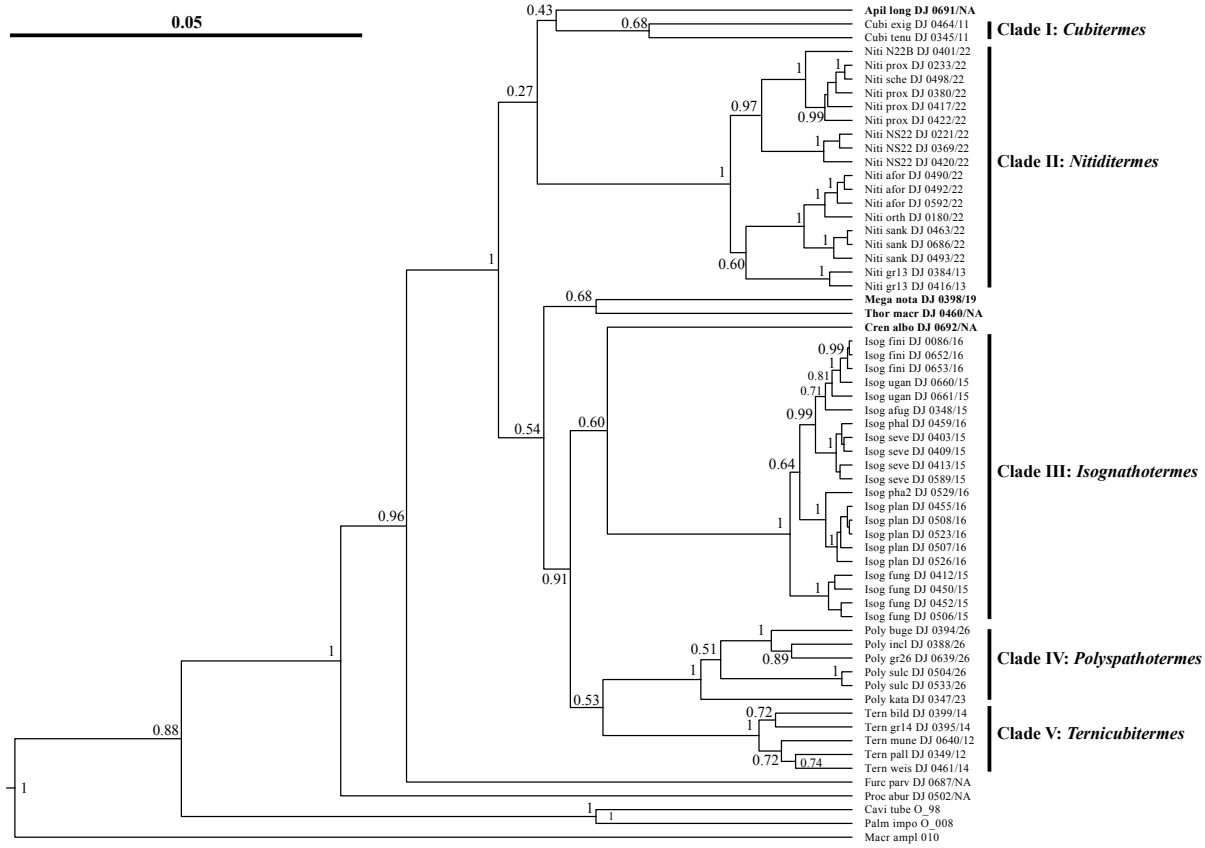

(S2B) Two-gene analysis: nuclear tree (*28S rDNA*)

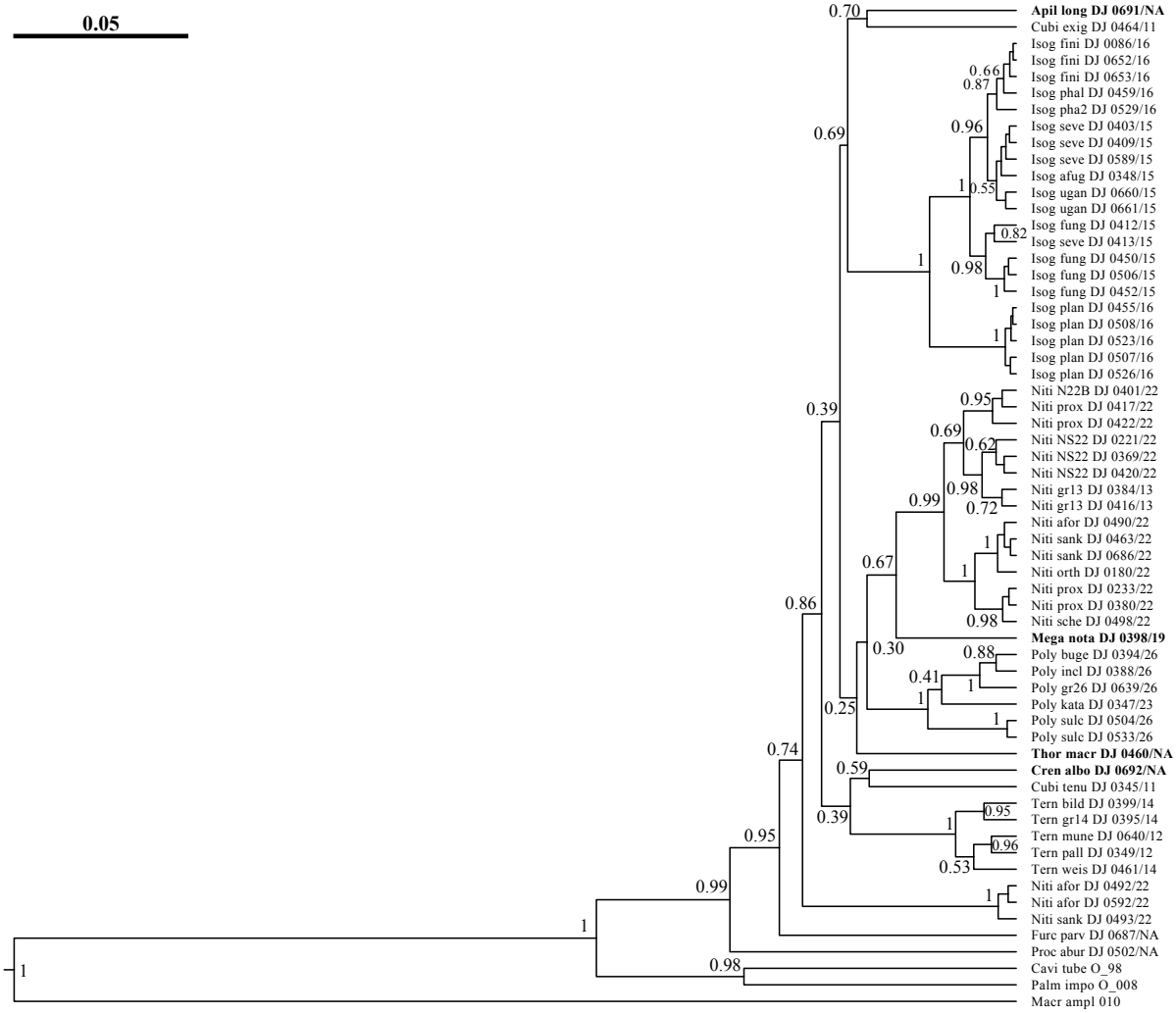

(S2C) Two-gene analysis: cophyloplot

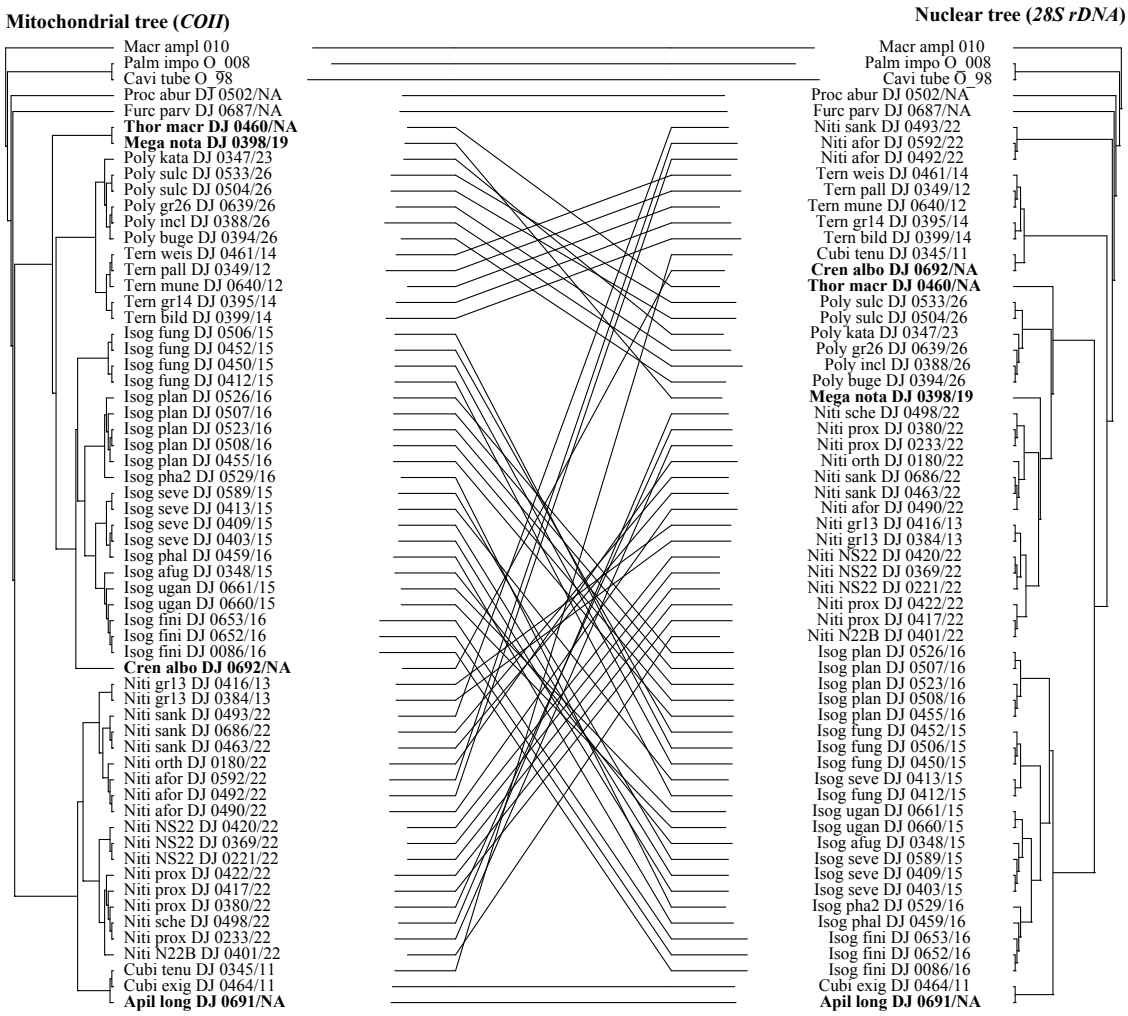

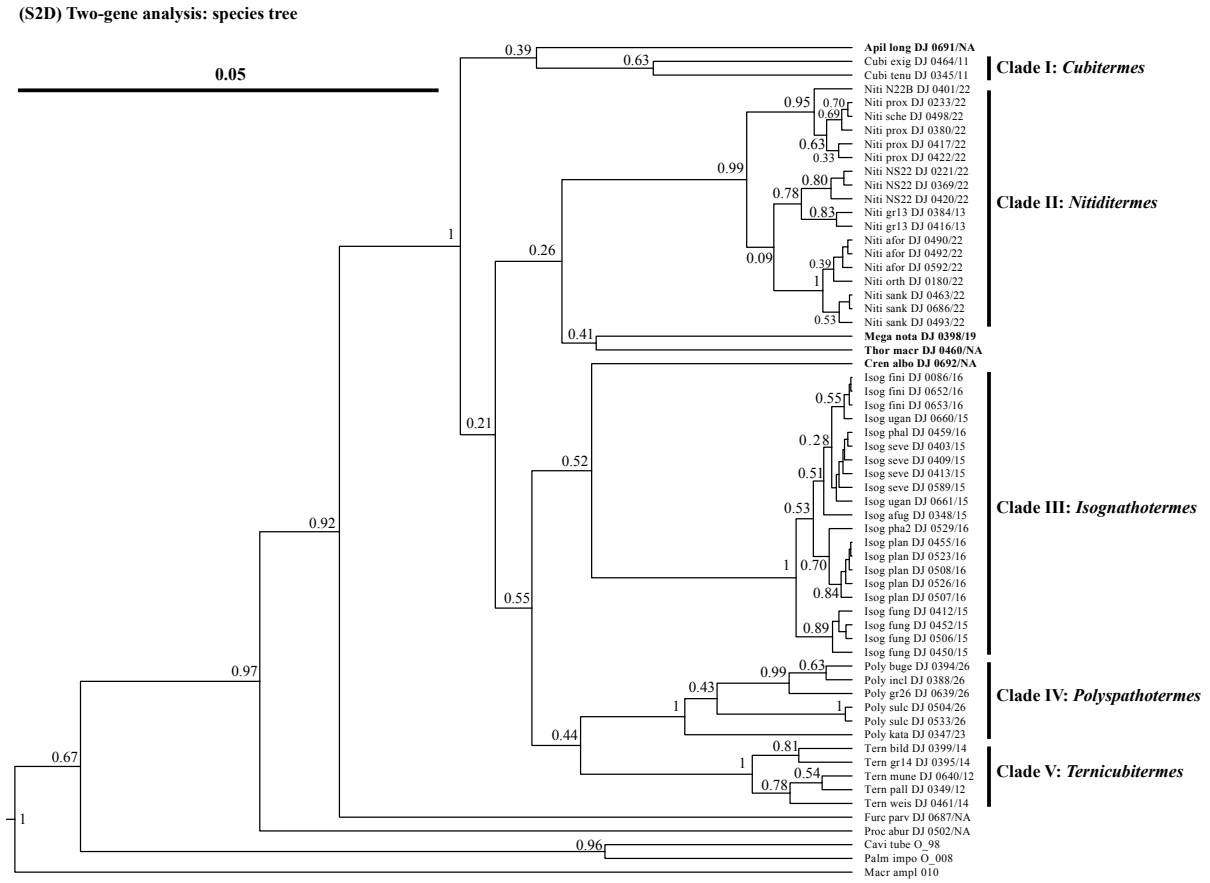

Fig. S2. Maximum clade credibility ultrametric gene and species trees resulting from Bayesian inference using the StarBEAST2 method for the two-gene dataset (mitochondrial *COII* and nuclear *28S rDNA*; 61 sequences): (**A**) mitochondrial and (**B**) nuclear trees, (**C**) a cophyloplot showing the incongruence between the two trees, and (**D**) the total evidence tree. Node support values are Bayesian posterior probabilities (BPP). Scale bar indicates the mean number of substitutions per site. Genera which previously made *Cubitermes* paraphyletic are indicated in bold.

B. Supplementary Methods SM-1: Molecular procedures

Total DNA was extracted from termite heads using a NucleoSpin Tissue kit (Macherey-Nagel). A fragment of ~650 bp of the *COI* was amplified using the universal forward LCO (LCO1490) and the reverse HCO (HCO2198) primers (Folmer *et al.* 1994), a fragment of ~680 bp of the *COII* with the modified forward primer A-tLeu (Miura *et al.* 2000) and the reverse primer B-tLys (Simon *et al.* 1994), and a fragment of ~840 bp of the *28S rDNA* with the forward Rd1.2a and reverse Rd4.2b primers (Whiting 2002). Amplification of each fragment was carried in 25 µL reactions containing 0.5 µL (1 U) MyTaq DNA polymerase (Bioline GmbH, Germany), 5 µL 5x MyTaq Reaction Buffer, 0.5 µL of each forward and reverse primer (20 µM of each), 1.5 µL of template DNA and PCR-grade water (q.s.). Cycling conditions used in this study are given in Table S2. A fraction of the amplification products was screened by electrophoresis on a 1% agarose gel and another fraction was purified with the Nucleofast PCR purification kit (Macherey-Nagel). Purified amplicons were sequenced with BigDye Terminator Cycle Sequencing kit v3.1. (Applied Biosystems) in 11.2 µL reactions containing 1.0 µL BigDye, 2.1 µL 5x Sequencing Buffer, 0.1 µL of forward or reverse primer (20 µM of each), 3-8 µL of amplicon and PCR-grade water (q.s.). Cycling conditions were as follow: an initial denaturing step at 96°C for 1 min, 25 cycles of denaturing at 96°C for 10 s, annealing at 50°C for 5 s, and extension at 60°C for 4 min. Sequencing products were purified with an ethanol/EDTA/sodium acetate method. Sequence data were obtained with an ABI 3730 Genetic Analyzer (Applied Biosystems) and were visualized and edited using the software CodonCode Aligner v8.0.2 (CodonCode Corporation, Dedham, MA.).

C. Supplementary Tables

Table S1: Samples used in this study with corresponding GenBank accessions of amplified genes.

Collection code	Code in this study	Species	Country; Locality	Latitude; Longitude (°)	Elevation (m.)	Collecting date	Collector	*COI*	*COII*	*28S rDNA*
CGO_073	Apil long DJ 0691/NA	*Apilitermes longiceps*	Rep. of the Congo; Mokabi	3.15 N; 16.97 E	528	3-Dec-17	Y. Roisin	MN646697	MN685897	MN685957
O_98	Cavi tube O98	*Cavitermes tuberosus*	French Guiana; Petit Saut	5.07 N; 52.98 W	75	19-Oct-14	S. Hellemans	MN646698	MF953242	MN685958
CMRT 176	Cren albo DJ 0692/NA	*Crenetermes albotarsalis*	Cameroon; Nyong river-left bank	3.41 N; 11.46 E	652	31-May-17	Y. Roisin	MN646699	MN685898	MN685959
9 RNAL Kin	Cubi exig DJ 0464/11	*Cubitermes exiguus*	Dem. Rep. of the Congo; Kinshasa, Unikin campus	4.43 S; 15.31 E	450	24-Apr-17	C. Kifukieto	MN646707	MN685909	MN685970
10 RNA K	Cubi tenu DJ 0345/11	*Cubitermes tenuiceps*	Dem. Rep. of the Congo; Mikembo-Kisangwe	11.49 S; 27.66 E	1200	1-Jun-16	P. Kasangij	MN646741	MN685946	MN686007
8 RNAL Bip	Furc parv DJ 0687/NA	*Furculitermes parviceps*	Cameroon; Bipindi	3.05 N; 10.47 E	100	23-Nov-16	P. Akama	MN646744	MN685950	MN686011
8 RNA K	Isog afug DJ 0348/15	*Isognathotermes* sp. aff. *ugandensis*	Dem. Rep. of the Congo; Mikembo-Kisangwe	11.49 S; 27.66 E	1200	1-Jun-16	P. Kasangij	MN646704	MN685906	MN685967
RDCT 17	Isog fini DJ 0086/16	*Isognathotermes finitimus*	Dem. Rep. of the Congo; Yangambi	0.88 N; 24.33 E	470	7-Jul-13	Y. Roisin	MN646708	MN685910	MN685971
RDCT 1	Isog fini DJ 0652/16	*Isognathotermes finitimus*	Dem. Rep. of the Congo; Yangambi	0.79 N; 24.52 E	470	5-Jul-13	Y. Roisin	MN646709	MN685911	MN685972
RDCT 143	Isog fini DJ 0653/16	*Isognathotermes finitimus*	Dem. Rep. of the Congo; Yangambi	0.80 N; 24.49 E	470	15-Jul-13	Y. Roisin	MN646710	MN685912	MN685973
RNAL 30	Isog fung DJ 0412/15	*Isognathotermes fungifaber*	Côte d'Ivoire; Banco forest	5.38 N; 4.06 W	70	17-Feb-15	G. Josens	MN646711	MN685913	MN685974
1 RNAL Mbo	Isog fung DJ 0450/15	*Isognathotermes fungifaber*	Cameroon; Mbongé	4.54 N; 9.11 E	40	30-Nov-16	P. Akama	MN646712	MN685914	MN685975
5 RNAL Bip	Isog fung DJ 0452/15	*Isognathotermes fungifaber*	Cameroon; Bipindi	3.05 N; 10.47 E	100	23-Nov-16	P. Akama	MN646713	MN685915	MN685976
CMRT 026	Isog fung DJ 0506/15	*Isognathotermes fungifaber*	Cameroon; Ebogo	3.38 N; 11.46 E	660	23-May-17	Y. Roisin	MN646714	MN685916	MN685977
CGO_036	Isog pha2 DJ 0529/16	*Isognathotermes* sp. pha2	Rep. of the Congo; Loundoungou	2.38 N; 17.07 E	490	4-Dec-17	Y. Roisin	MN646722	MN685925	MN685986
2 RNAL Kin	Isog phal DJ 0459/16	*Isognathotermes* sp. phal	Dem. Rep. of the Congo; Luméné gallery on Batéké Plateau	4.43 S; 16.05 E	550	22-Apr-17	C. Kifukieto	MN646723	MN685926	MN685987
4 RNAL GA	Isog plan DJ 0455/16	*Isognathotermes planifrons*	Gabon; Nkobissimo	2.24 N; 11.49 E	600	15-Apr-17	G. Trembleau	MN646724	MN685927	MN685988
CMRT 154	Isog plan DJ 0507/16	*Isognathotermes planifrons*	Cameroon; Akometa	3.47 N; 11.55 E	675	6-Jun-17	Y. Roisin	MN646725	MN685928	MN685989
CMRT 100	Isog plan DJ 0508/16	*Isognathotermes planifrons*	Cameroon; Yolo-Chimpa	5.59 N; 10.89 E	1200	30-May-17	Y. Roisin	MN646726	MN685929	MN685990

ELECTRONIC SUPPLEMENTARY MATERIALS

Collection code	Code in this study	Species	Country; Locality	Latitude; Longitude (°)	Elevation (m.)	Collecting date	Collector	*COI*	*COII*	*28S rDNA*
CGO_059	Isog plan DJ 0523/16	*Isognathotermes planifrons*	Rep. of the Congo; Mokabi	3.15 N; 16.96 E	530	6-Dec-17	Y. Roisin	MN646727	MN685930	MN685991
CGO_008	Isog plan DJ 0526/16	*Isognathotermes planifrons*	Rep. of the Congo; Loundoungou	2.38 N; 17.07 E	455	3-Dec-17	Y. Roisin	MN646728	MN685931	MN685992
7 RNAL BE	Isog seve DJ 0403/15	*Isognathotermes severus*	Benin; Birni forest	10.02 N; 1.53 E	200	1-Nov-16	L.E. Loko	MN646735	MN685940	MN686001
7 RCI	Isog seve DJ 0409/15	*Isognathotermes severus*	Côte d'Ivoire; Taabo	6.30 N; 5.00 W	140	21-Feb-15	G. Josens	MN646736	MN685941	MN686002
50 RCI	Isog seve DJ 0413/15	*Isognathotermes severus*	Côte d'Ivoire; Man-Duékoué road	6.83 N; 7.41 W	250	1-Mar-15	G. Josens	MN646737	MN685942	MN686003
6 RNAL CA	Isog seve DJ 0589/15	*Isognathotermes severus*	Central African Rep.; Bondoé	5.17 N; 17.74 E	700	26-Apr-18	S.P. Wango	MN646738	MN685943	MN686004
BDIT 105	Isog ugan DJ 0660/15	*Isognathotermes ugandensis*	Burundi; Ruvubu N.P.	2.95 S; 30.43 E	1500	29-Nov-13	Y. Roisin	NA	MN685947	MN686008
BDIT 88	Isog ugan DJ 0661/15	*Isognathotermes ugandensis*	Burundi; Gihofi-Giharo road pk 75	3.99 S; 30.15 E	1200	27-Nov-13	Y. Roisin	MN646742	MN685948	MN686009
CGO_010	Macr ampl 010	*Macrotermes amplus*	Rep. of the Congo; Loundoungou	2.38 N; 17.07 E	462	3-Dec-17	Y. Roisin	MN646745	MN685951	MN686012
RNAL 57	Mega nota DJ 0398/19	*Megagnathotermes notandus*	Côte d'Ivoire; Torogo	9.38 N; 5.63 W	330	26-Feb-15	G. Josens	MN646747	MN685953	MN686014
CMRT 082	Niti afor DJ 0490/22	*Nititidermes* sp. aff. *orthognathus*	Cameroon; Koutaba	5.62 N; 10.75 E	1200	29-May-17	Y. Roisin	NA	MN685903	MN685964
CMRT 113	Niti afor DJ 0492/22	*Nititidermes* sp. aff. *orthognathus*	Cameroon; Koutaba-Manchi road	5.60 N; 10.75 E	1150	31-May-17	Y. Roisin	NA	MN685904	MN685965
3 RNAL CA	Niti afor DJ 0592/22	*Nititidermes* sp. aff. *orthognathus*	Central African Rep.; Bondoé	5.17 N; 17.74 E	700	26-Apr-18	S.P. Wango	NA	MN685905	MN685966
11 RNAL BF	Niti gr13 DJ 0384/13	*Nititidermes* sp. gr13	Burkina Faso; Tiogo	12.19 N; 2.71 W	280	1-Aug-16	S. Traoré	MN646715	MN685917	MN685978
01 SE	Niti gr13 DJ 0416/13	*Nititidermes* sp. gr13	Senegal; Diouroup	14.38 N; 16.54 W	10	19-Nov-16	A. Ndiaye	MN646716	MN685918	MN685979
4 RNAL BE	Niti N22B DJ 0401/22	*Nititidermes* sp. N22B	Benin; Birni forest	10.02 N; 1.53 E	400	1-Nov-16	L.E. Loko	MN646700	MN685899	MN685960
70 RCI	Niti NS22 DJ 0221/22	*Nititidermes* sp. NS22	Côte d'Ivoire; Toumodi	6.60 N; 5.08 W	195	25-Feb-15	G. Josens	MN646701	MN685900	MN685961
3 RNAL BF	Niti NS22 DJ 0369/22	*Nititidermes* sp. NS22	Burkina Faso; Bekuy	11.61 N; 3.91 W	300	1-Aug-16	S. Traoré	MN646702	MN685901	MN685962
05 SE	Niti NS22 DJ 0420/22	*Nititidermes* sp. NS22	Senegal; Indiga, on Tambacounda road	12.60 N; 12.22 W	150	22-Nov-16	A. Ndiaye	MN646703	MN685902	MN685963
BDIT 91	Niti orth DJ 0180/22	*Nititidermes orthognathus*	Burundi; Gihofi-Giharo road pk 76	3.98 S; 30.16 E	1200	27-Nov-13	Y. Roisin	MN646720	MN685923	MN685984
RNAL 59	Niti prox DJ 0233/22	*Nititidermes proximatus*	Côte d'Ivoire; Danané-Man road	7.28 N; 7.77 W	330	28-Feb-15	G. Josens	MN646729	MN685932	MN685993

ELECTRONIC SUPPLEMENTARY MATERIALS

Collection code	Code in this study	Species	Country; Locality	Latitude; Longitude (°)	Elevation (m.)	Collecting date	Collector	*COI*	*COII*	*28S rDNA*
6 RNAL BF	Niti prox DJ 0380/22	*Nititermes proximatus*	Burkina Faso; Bobo Dioulasso	11.21 N; 4.39 W	400	1-Aug-16	S. Traoré	MN646730	MN685933	MN685994
02 SE	Niti prox DJ 0417/22	*Nititermes proximatus*	Senegal; Dienoudiala	13.19 N; 13.05 W	80	22-Nov-16	A. Ndiaye	MN646731	MN685934	MN685995
07 SE	Niti prox DJ 0422/22	*Nititermes proximatus*	Senegal; Samékouta-Kédougou	12.61 N; 12.11 W	130	22-Nov-16	A. Ndiaye	MN646732	MN685935	MN685996
5 RNAL Kin	Niti sank DJ 0463/22	*Nititermes sankurensis*	Dem. Rep. of the Congo; Batéké Plateau	4.39 S; 16.07 E	660	23-Apr-17	C. Kifukieto	NA	MN685936	MN685997
CMRT 117	Niti sank DJ 0493/22	*Nititermes sankurensis*	Cameroon; Koutaba-Manchi road	5.61 N; 10.75 E	1150	31-May-17	Y. Roisin	MN646733	MN685937	MN685998
6 RNAL Kin	Niti sank DJ 0686/22	*Nititermes sankurensis*	Dem. Rep. of the Congo; Batéké Plateau	4.39 S; 16.08 E	660	23-Apr-17	C. Kifukieto	NA	MN685938	MN685999
71 RCI	Niti sche DJ 0498/22	*Nititermes schereri*	Côte d'Ivoire; Man	7.41 N; 7.59 W	450	27-Feb-15	G. Josens	MN646734	MN685939	MN686000
O_008	Palm impo O008	*Palmitermes impostor*	French Guiana; Petit Saut	5.07 N; 52.98 W	82	15-Nov-15	S. Hellemans	MN646748	MN685954	MN686015
BH353	Poly buge DJ 0394/26	*Polyspathotermes bugeserae*	Burundi; Ruvubu N.P.	2.95 S; 30.48 E	1500	30-Sep-14	B. Host	MN646706	MN685908	MN685969
2 RNAL ZA	Poly gr26 DJ 0639/26	*Polyspathotermes* sp. gr26	Dem. Rep. of the Congo; South of Moero Lake	9.68 S; 28.58 E	930	23-Nov-18	P. Kasangij	MN646717	MN685920	MN685981
6 RNA K	Poly incl DJ 0388/26	*Polyspathotermes inclitus*	Dem. Rep. of the Congo; Mikembo-Kisangwe	11.49 S; 27.66 E	1200	1-Jun-16	P. Kasangij	MN646718	MN685921	MN685982
4 RNA K	Poly kata DJ 0347/23	*Polyspathotermes katangensis*	Dem. Rep. of the Congo; Mikembo-Kisangwe	11.49 S; 27.66 E	1200	1-Jun-16	P. Kasangij	MN646746	MN685952	MN686013
CMRT 015	Poly sulc DJ 0504/26	*Polyspathotermes sulcifrons*	Cameroon; Ebogo	3.38 N; 11.46 E	660	22-May-17	Y. Roisin	MN646739	MN685944	MN686005
CGO_075	Poly sulc DJ 0533/26	*Polyspathotermes sulcifrons*	Rep. of the Congo; Mokabi	3.15 N; 16.96 E	530	9-Dec-17	Y. Roisin	MN646740	MN685945	MN686006
29 RCI	Proc abur DJ 0502/NA	*Procubitermes aburiensis*	Côte d'Ivoire; Lamto-Pakobo	6.22 N; 5.03 W	120	21-Feb-15	G. Josens	MN646749	MN685955	MN686016
RNAL 39	Tern bild DJ 0399/14	*Ternicubitermes bilobatodes*	Côte d'Ivoire; Youhouli	5.44 N; 4.49 W	100	18-Feb-15	G. Josens	MN646705	MN685907	MN685968
BH343	Tern gr14 DJ 0395/14	*Ternicubitermes* sp. gr14	Burundi; Ruvubu N.P.	2.95 S; 30.44 E	1500	30-Sep-14	B. Host	NA	MN685919	MN685980
3 RNAL ZA	Tern mune DJ 0640/12	*Ternicubitermes muneris*	Dem. Rep. of the Congo; South of Moero Lake	9.68 S; 28.54 E	930	23-Nov-18	P. Kasangij	MN646719	MN685922	MN685983
1 RNA K	Tern pall DJ 0349/12	*Ternicubitermes pallidiceps*	Dem. Rep. of the Congo; Mikembo-Kisangwe	11.49 S; 27.66 E	1200	1-Jun-16	P. Kasangij	MN646721	MN685924	MN685985
3 RNAL Kin	Tern weis DJ 0461/14	*Ternicubitermes weissi*	Dem. Rep. of the Congo; Batéké Plateau	4.39 S; 16.08 E	660	22-Apr-17	C. Kifukieto	MN646743	MN685949	MN686010
1 RNAL Kin	Thor macr DJ 0460/NA	*Thoracotermes macrothorax*	Dem. Rep. of the Congo; Luméné gallery on Batéké Plateau	4.43 S; 16.05 E	550	23-Apr-17	C. Kifukieto	MN646750	MN685956	MN686017

Table S2: Primers and cycling conditions used in this study.

Gene	Primer name	Sequence (5'-3')	Reference	Cycling conditions	Initial denaturation	Denaturation	Annealing	Extension	Final extension	Number of cycles
COI	LCO1490	GGT CAA CAA ATC ATA AAG ATA TTG G	Folmer *et al.*, 1994	**T (°C)**	94	94	47	72	72	40
	HCO2198	TAA ACT TCA GGG TGA CCA AAA AAT CA	Folmer *et al.*, 1994	**t (s)**	120	60	60	75	420	
COII	Mod A-tLeu	CAG ATA AGT GCA TTG GAT TT	Miura *et al.*, 2000	**T (°C)**	94	94	45	72	72	35
	B-tLys	GTT TAA GAG ACC AGT ACT TG	Simon *et al.*, 1994	**t (s)**	180	30	30	60	600	
28S rDNA	Rd1.2a	CCC SSG TAA TTT AAG CAT ATT A	Whiting, 2002	**T (°C)**	94	94	44	72	72	40
	Rd4.2b	CCT TGG TCC GTG TTT CAA GAC GG	Whiting, 2002	**t (s)**	120	60	60	75	420	

Table S3: *COII* sequences retrieved from GenBank for the construction of the MrBayes non-ultrametric tree, and re-identification of species prior to the splitting of *Cubitermes* into new genera. Abbreviations: DRC, Democratic Republic of the Congo; N. P., National Park.

Collection code	Code in this study	Identification in original publication	Identification revised	Locality	Accession	Original publication
RDCT183	Apil long DJ 0702/NA KY224419	*Apilitermes longiceps*	*Apilitermes longiceps*	DRC Yangambi	KY224419	Bourguignon *et al*. (2017)
O_98	Cavi tube O_98	*Cavitermes tuberosus*	*Cavitermes tuberosus*	French Guiana Petit Saut	MF953242	Hellemans *et al.* (2019)
RDCT129	Cren albo DJ 0700/NA KY224620	*Crenetermes albotarsalis*	*Crenetermes albotarsalis*	DRC Yangambi	KY224620	Bourguignon *et al*. (2017)
CA1	Isog sp_C KP026265	*Cubitermes fungifaber*	*Isognathotermes* "spC"	Cameroon, Mbalmayo	KP026265	Bourguignon *et al*. (2015)
ROCT46	Isog sp_C DJ 0631/16 DQ127306	*Cubitermes* sp. *affinis subarquatus* "spC"	*Isognathotermes* "spC"	Gabon Rocher (Lopé N. P.)	DQ127306	Roy *et al*. (2006)
RDCT220	Isog fini DJ 0620/16 KY224569	*Cubitermes* sp A	*Isognathotermes finitimus*	DRC Yangambi	KY224569	Bourguignon *et al*. (2017)
ROCT16	Isog fung DJ 0623/15 DQ127302	*Cubitermes* sp. *affinis subarquatus* "spA"	*Isognathotermes fungifaber*	Gabon Rocher (Lopé N. P.)	DQ127302	Roy *et al*. (2006)
DODTD2	Isog fung DJ 0625/15 DQ246541	*Cubitermes* sp. *affinis subarquatus* "spD"	*Isognathotermes fungifaber*	Gabon Doda (Lopé N. P.)	DQ246541	Roy *et al*. (2006)
OKOT26	Isog plan DJ 0624/16 DQ127312	*Cubitermes* sp. *affinis subarquatus* "spB"	*Isognathotermes planifrons*	Gabon Okoumé (Lopé N. P.)	DQ127312	Roy *et al*. (2006)
BDIT078	Isog ugan DJ 0091/15 KY224661	*Cubitermes ugandensis*	*Isognathotermes ugandensis*	Burundi Mahanga	KY224661	Bourguignon *et al*. (2017)
BDIT069	Niti fulv DJ 0183/22 KY224600	*Cubitermes* nr. *fulvus*	*Nitiditermes fulvus*	Burundi Buga	KY224600	Bourguignon *et al*. (2017)
BDIT106	Poly katb DJ 0093/23 KY224475	*Cubitermes oblectatus*	*Polyspathotermes* sp. aff. *katangensis*	Burundi Ruvubu N. P.	KY224475	Bourguignon *et al*. (2017)
BDIT075	Poly buge DJ 0186/26 KY224421	*Cubitermes fulvus*	*Polyspathotermes bugeserae*	Burundi Mahanga	KY224421	Bourguignon *et al*. (2017)
RDCT130	Poly sulc DJ 0676/26 KY224606	*Cubitermes sulcifrons*	*Polyspathotermes sulcifrons*	DRC Yangambi	KY224606	Bourguignon *et al*. (2017)
RDCT128	Thor macr DJ 0701/NA KY224714	*Thoracotermes macrothorax*	*Thoracotermes macrothorax*	DRC Yangambi	KY224714	Bourguignon *et al*. (2017)

Table S4: List of valid names of the taxa formerly included (as in Krishna *et al.* 2013c) in the genera *Cubitermes*, *Megagnathotermes* and *Nitiditermes*. Asterisks indicate type species. Indented names are synonyms. With the exception of *Polyspathotermes katangensis* (transferred from *Megagnathotermes*) and the type species of *Megagnathotermes* and *Nitiditermes* (unchanged), all species were formerly in the genus *Cubitermes*.

***Cubitermes* Wasmann, 1906**
**Cubitermes bilobatus* (Haviland, 1898)
    C. bilobatus curtus Sjöstedt, 1926
Cubitermes conjenii (Fuller, 1925)
Cubitermes exiguus Mathot, 1964
Cubitermes pretorianus Silvestri, 1914
Cubitermes pretorianus heidelbergi Fuller, 1925
Cubitermes sanctaeluciae (Fuller, 1925)
Cubitermes tenuiceps (Sjöstedt, 1913)
Cubitermes transvaalensis (Fuller, 1925)
Cubitermes zulucola Sjöstedt, 1924
    C. pseudoduplex (Fuller, 1925)

***Isognathotermes* Sjöstedt, 1926**
Isognathotermes bulbifrons (Sjöstedt, 1924)
    I. heghi (Sjöstedt, 1924)
Isognathotermes congoensis (Emerson, 1928)
Isognathotermes finitimus (Schmitz, 1915)
    I. loubetsiensis (Sjöstedt, 1924)
    I. subarquatus (Sjöstedt, 1926)
Isognathotermes fungifaber (Sjöstedt, 1896)
    I. banksi (Emerson, 1928)
    I. comstocki (Emerson, 1928)
    I. schmidti (Emerson, 1928)
Isognathotermes gaigei (Emerson, 1928)
Isognathotermes gibbifrons (Sjöstedt, 1924)
Isognathotermes kemneri (Emerson, 1928)
**Isognathotermes minitabundus* (Sjöstedt, 1913)
Isognathotermes modestior (Silvestri, 1914)
Isognathotermes planifrons (Sjöstedt, 1924)
    ? I. fungifaber elongatus (Sjöstedt, 1924)
Isognathotermes severus (Silvestri, 1914)
Isognathotermes silvestrii (Sjöstedt, 1925)
Isognathotermes speciosus (Sjöstedt, 1924)
Isognathotermes ugandensis (Fuller, 1923)
    I. antennalis (Sjöstedt, 1924)
Isognathotermes zenkeri (Desneux, 1904)

***Megagnathotermes* Silvestri, 1914**
**Megagnathotermes notandus* Silvestri, 1914

Nititermes **Emerson, 1960**
Nititermes aemulus (Silvestri, 1914)
Nititermes anatruncatus (Fuller, 1925)
**Nititermes berghei* Emerson, 1960
Nititermes curtatus (Silvestri, 1914)
Nititermes fulvus (Williams, 1966)
Nititermes niokoloensis (Roy-Noël, 1969)
Nititermes oculatus (Silvestri, 1914)
Nititermes orthognathus (Emerson, 1928)
Nititermes proximatus (Silvestri, 1914)
Nititermes sankurensis (Wasmann, 1911)
    N. cubicephalus (Sjöstedt, 1913)
    N. sankurensis elongatus (Sjöstedt, 1926)
    N. sibitiensis (Sjöstedt, 1925)
Nititermes schereri (von Rosen, 1912)
Nititermes sierraleonicus (Sjöstedt, 1911)
Nititermes testaceus (Williams, 1966)
Nititermes truncatoides (Fuller, 1925)
    N. truncatoides sordwana (Fuller, 1925)
Nititermes truncatus (Holmgren, 1913)
    N. duplex nduma (Fuller, 1925)

Polyspathotermes **Josens & Deligne, gen. nov.**
Polyspathotermes bugeserae (Bouillon & Vincke, 1971)
Polyspathotermes inclitus (Silvestri, 1912)
    P. domifaber (Sjöstedt, 1913)
Polyspathotermes intercalatus (Silvestri, 1914)
    P. hamatus (Sjöstedt, 1926)
Polyspathotermes katangensis (Sjöstedt, 1927)
Polyspathotermes montanus (Williams, 1966)
Polyspathotermes oblectatus (Harris, 1958)
**Polyspathotermes sulcifrons* (Wasmann, 1911)
Polyspathotermes umbratus (Williams, 1954)

Ternicubitermes **Josens & Deligne, gen. nov.**
**Ternicubitermes bilobatodes* (Silvestri, 1912)
Ternicubitermes breviceps (Sjöstedt, 1913)
Ternicubitermes duplex (Holmgren, 1913)
Ternicubitermes falcifer (Williams, 1966)
Ternicubitermes glebae (Sjöstedt, 1913)
Ternicubitermes latens (Williams, 1966)
Ternicubitermes microduplex (Fuller, 1925)
Ternicubitermes muneris (Sjöstedt, 1913)
    T. bisulcatus (Sjöstedt, 1914)
Ternicubitermes pallidiceps (Sjöstedt, 1913)
Ternicubitermes subcrenulatus (Silvestri, 1914)
Ternicubitermes undulatus (Fuller, 1925)
Ternicubitermes weissi (Silvestri, 1912)
Ternicubitermes zavattarii (Ghidini, 1937)

D. Supplementary References

Folmer, O., Black, M., Hoeh, W., Lutz, R., and Vrijenhoek, R. (1994). DNA primers for amplification of mitochondrial cytochrome c oxidase subunit I from diverse metazoan invertebrates. *Molecular Marine Biology and Biotechnology* **3**, 294–299. doi:10.1371/journal.pone.0013102

Hellemans, S., Kaczmarek, N., Marynowska, M., Calusinska, M., Roisin, Y., Fournier, D. (2019). Bacteriome-associated *Wolbachia* of the parthenogenetic termite *Cavitermes tuberosus*. *FEMS Microbiology Ecology* **95**, fiy235. doi:10.1093/femsec/fiy235

Miura, T., Roisin, Y., and Matsumoto, T. (2000). Molecular phylogeny and biogeography of the nasute termite genus *Nasutitermes* (Isoptera: Termitidae) in the Pacific tropics. *Molecular Phylogenetics and Evolution* **17**, 1–10. doi:10.1006/mpev.2000.0790

Simon, C., Frati, F., Beckenbach, A., Crespi, B., Liu, H., and Flook, P. (1994). Evolution, weighting, and phylogenetic utility of mitochondrial gene sequences and a compilation of conserved polymerase chain reaction primers. *Annals of the Entomological Society of America* **87**, 651–701. doi:10.1080/17470210902990829

Whiting, M. F. (2002). Mecoptera is paraphyletic: multiple genes and phylogeny of Mecoptera and Siphonaptera. *Zoologica Scripta* **31**, 93–104. doi:10.1046/j.0300-3256.2001.00095.x